

青藏高原东南缘兰坪—思茅地体晚始新世以来差异性地壳变形的成因讨论

杨向东^{1,2)}, 全亚博^{1,2)}, 王恒³⁾, 裴军令^{1,2)}, 孙欣欣⁴⁾, 王晨旭^{1,2)}, 杨振宇⁴⁾

1) 中国地质科学院地质力学研究所, 北京, 100081;

2) 自然资源部古地磁与古构造重建重点实验室, 北京, 100081;

3) 中国地震局地质研究所, 北京, 100029; 4) 首都师范大学资源环境与旅游学院, 北京, 100048

内容提要:印支地块北部地壳的侧向挤出逃逸方式和动力机制仍存在争议,本文通过兰坪盆地晚始新世红层的构造磁学和磁倾角偏矫研究,探讨了青藏高原东南缘大陆变形的成因等关键问题。磁倾角偏矫后的原生特征剩磁分量为 $D_s = 264.5^\circ, I_s = -39.4^\circ, k = 21.4, \alpha_{95} = 9.6^\circ, N = 12$ 。结果表明自晚始新世以来,位于印支地块西北部的兰坪—思茅地体,其北部相对于东亚古地磁参考极发生了 $80.3^\circ \pm 8.9^\circ$ 的顺时针旋转运动,同时发生了 $5.8^\circ \pm 7.2^\circ$ (638 ± 792 km) 的不显著南向运动。综合前人的古地磁研究结果,表明兰坪—思茅地体北部和中部地区存在显著的差异性旋转变形。本文提出地体北部~ 80° 的顺时针旋转变形与印度板块东端和西缅甸地块向北楔入欧亚大陆联合作用造成的北东—东向挤压作用相关,而地体中部复杂的差异性旋转变形则与川滇地体的南向挤压和临沧花岗岩带的阻挡作用所导致的局部地壳构造变形相关。因此,兰坪—思茅地体北部和中部的差异性旋转运动是地体整体性顺时针旋转运动和局部差异性旋转变形相叠加的结果,与下地壳粘性通道流的驱动并无直接关联,而与相邻地块间的差异性运动所导致的地块间的挤压作用相关。自晚始新世以来,在兰坪—思茅地体北部地区上地壳沿大型走滑断裂带发生的东南向挤出逃逸运动和下地壳通道流所导致的上地壳韧性变形作用可能共存,而地体中南部地区沿大形走滑断裂带发生整体性侧向挤出逃逸模型可能占据主导地位。

关键词:青藏高原东南缘;兰坪—思茅地体;始新世;古地磁;侧向旋转挤出逃逸;磁倾角偏低

自早古近纪印度板块和欧亚大陆发生初始碰撞以来,印度板块持续北向挤压欧亚大陆,导致东亚在新生代经历了强烈的地壳变形,不仅在青藏高原内部及周缘形成了一系列巨大的近东西向展布的山系,还在青藏高原周缘形成了一系列大型走滑断裂系(Molnar and Tapponnier, 1975; Tapponnier et al., 1982, 1986; Klootwijk et al., 1985; Beck et al., 1995; Yin An et al., 2000, 2006; Tong Yabo et al., 2008; Najman et al., 2010; Van Hinsbergen et al., 2012)。近30年来在青藏高原及周缘地区进行的构造地质学及地球物理学研究认为,印度与欧亚大陆初始碰撞以来,欧亚大陆内部发生了约 $780 \sim 1740$ km 的纬向地壳缩短(Yin An et al., 2000, 2006; Huang Baochun et al., 2005; Molnar and Stock,

2009; Copley et al., 2010; Dupont-Nivet et al., 2010; Liebke et al., 2010; Van Hinsbergen et al., 2011; Cogné et al., 2013; Ma Yiming et al., 2014; Li Zhenyu et al., 2015; Yang Tianshui et al., 2015; Yi Zhiyu et al., 2015; Cao Yong et al., 2017; Li Shihu et al., 2017; Tong Yabo et al., 2017)。这一巨大的纬向缩短量部分由青藏高原内部一系列新生代逆冲推覆构造和褶皱系所吸收,如冈底斯冲断带(Harrison et al., 1992; Yin An et al., 1994),狮泉河—改则—安多逆冲断裂系及风火山—囊谦褶皱系等(Dewey et al., 1988)。另一部分纬向地壳缩短普遍被认为由青藏高原及周缘地壳物质沿大型走滑断裂带发生的侧向挤出逃逸和旋转来协调(Tapponnier et al., 1982; Leloup et al., 1995;

注:本文为国家自然科学基金资助项目“晚白垩世以来四川盆地旋转运动及其对盆地边界构造带新生代构造演化的控制作用”(编号:41872221)、国家自然基金重大研究计划子课题“印度—亚洲碰撞过程拉萨地块和特提斯喜马拉雅地体的运动学研究”(编号:91855216)、中国地质科学院基本科研业务费项目“特提斯消亡过程多陆块单向裂解—汇聚研究”(编号:JYYWF20182102)的成果。

收稿日期:2020-01-01; 改回日期:2020-04-18; 责任编辑:刘志强。Doi:10.16509/j.georeview.2020.04.005

作者简介:杨向东,男,1995年生,硕士研究生,构造地质与古地磁学专业;Email:xdyangmy@163.com。通讯作者:全亚博,男,1981年生,博士,副研究员,主要从事构造地质与古地磁学研究;Email:tyb816@163.com。

Wang, 1998; Wang and Burchfiel, 2000; Molnar and Dayem, 2010)。例如,青藏高原北缘柴达木盆地沿阿尔金左旋走滑断裂带发生的北东向挤出(Yin An and Harrison, 2000);青藏高原东部松潘—甘孜地体东向挤出挤压四川盆地,并导致了形成于中生代的龙门山构造带的活化(Clark and Royden, 2000; Tapponnier et al., 2001; Xu Qiang et al., 2016; 张岳桥等, 2008, 2013);青藏高原东南缘印支地块、缅泰地块以及腾冲地块沿哀牢山—红河左旋走滑断裂带、高黎贡右旋韧性剪切带以及实楷右旋走滑断裂带发生的东南向挤出逃逸(Tapponnier et al., 1982, 2001; Leloup et al., 1995, 2001; Peltzer and Tapponnier, 1988; Replumaz and Tapponnier, 2003)。

定量分析青藏高原内部地壳挤压缩短变形和高原地壳侧向挤出逃逸对欧亚大陆新生代纬向地壳缩短的贡献量,是正确认识青藏高原隆升过程及其动力机制的关键。另外,青藏高原地壳物质侧向挤出逃逸运动对于认识高原周缘区域新生代地壳构造变形、大型走滑断裂系的构造演化、现代构造地貌及河流的塑造和演化过程都有着极为重要的意义。前人建立了两个基于高原周缘新生代地壳运动规律和地壳构造变形特征的终端构造演化模型:①青藏高原东南缘诸多刚性地块沿多条走滑断裂带的东向或东南向侧向挤出逃逸(Molnar and Tapponnier, 1975; Tapponnier et al., 1982, 2001; Peltzer and Tapponnier, 1988; Replumaz and Tapponnier, 2003);②青藏高原东南缘上地壳物质在下地壳粘性通道流的驱动下发生复杂的韧性变形(Clark and Royden, 2000; Shen Zhenkang et al., 2005; Royden et al., 2008)。这二个构造演化模型的主要分歧在于对高原周缘新生代地壳运动方式的不同论述:侧向挤出逃逸模型强调地壳块体大规模的南向运移,其间地块内部并没有发生显著的地壳构造变形,而下地壳粘性通道流模型则强调地块内部发生了强烈构造变形,其间地块并不一定伴随着显著的南向运移。为了验证这两个主流构造模型的合理性,众多学者在青藏高原东南缘这一地壳侧向挤出逃逸构造最为典型的区域进行了大量的古地磁学研究。近30年来,前人从位于印支地块北端的兰坪—思茅地体内部的白垩纪和古近纪红层中获得的大量古地磁数据表明,自约32 Ma,兰坪—思茅地体中南部以哀牢山—红河左旋走滑断裂系为构造边界,发生了约400~700 km的南向顺时针旋转挤出逃逸

(Funahara et al., 1992; Yang Zhenyu and Besse, 1993; Huang Kainian and Opdyke, 1993; 杨振宇等, 1998; Sato et al., 1999; Tapponnier et al., 2001; Tanaka et al., 2008; 张海峰等, 2012; Tong Yabo et al., 2013; Wang Heng et al., 2016; Li Shihu et al., 2017)。这些研究结果似乎倾向于支持刚性块体的侧向挤出模式。然而,从腾冲地块和保山地体内约40 Ma的火成岩中获得的原生特征剩磁分量,以及沉积岩中获得的晚渐新世/早中新世的重磁化剩磁分量都表明,两块体虽然相对于东亚古地磁极经历了极为显著的顺时针旋转变形(约80°),但并未发生显著的南向运移,其更倾向于下地壳粘性通道流模型(Kornfeld et al., 2014a, b; Tong Yabo et al., 2016)。即使在兰坪—思茅地体内部,白垩纪和新生代古地磁数据间也存在显著的不协调性。兰坪盆地内获得的始新世古地磁数据显示这一地区与保山地体类似,相对于东亚古地磁极经历了约80°的顺时针旋转,但似乎仅发生了小规模的南向运移(Sato et al., 2001; Tong Yabo et al., 2016; Li Shihu et al., 2017)。而从位于兰坪—思茅地体中部的云龙、下关等地区白垩系和古近系中获得的古地磁数据则显示这些区域经历了规模较小的顺时针旋转变形,但却伴随着极为显著的南向运移(Sato et al., 1999; Tanaka et al. 2008; Yang Zhenyu et al., 2001; 全亚博等, 2014)。这一差异性构造变形和地壳运动方式又暗示着青藏高原东南缘的新生代构造演化很可能主要受下地壳粘性流的驱动。

由于兰坪—思茅地体内部的古地磁数据全部来自白垩纪和古近纪红层,其潜在的由沉积压实作用所导致的磁倾角浅化现象可能会导致对地块纬向运移量的错误估算(Tan Xiaodong et al., 1996; Tauxe, 2005),从而导致兰坪—思茅地体北部和中部地区纬向运动间的差异性。基于这一重要问题,本次研究在兰坪—思茅地体北部的兰坪盆地内始新世红层中开展了详细的构造磁学研究及磁倾角浅化矫正分析,以精确估算兰坪—思茅地体北部在新生代所经历的差异性顺时针旋转量和纬向运移量,进而讨论兰坪—思茅地体新生代地壳侧向挤出逃逸方式和其动力机制。

1 地质背景与采样

兰坪—思茅地体位于印支地块的北部。崇山韧性剪切带—澜沧江缝合带构成了其与保山地体的构造边界,而金沙江—哀牢山—红河走滑断裂带构成

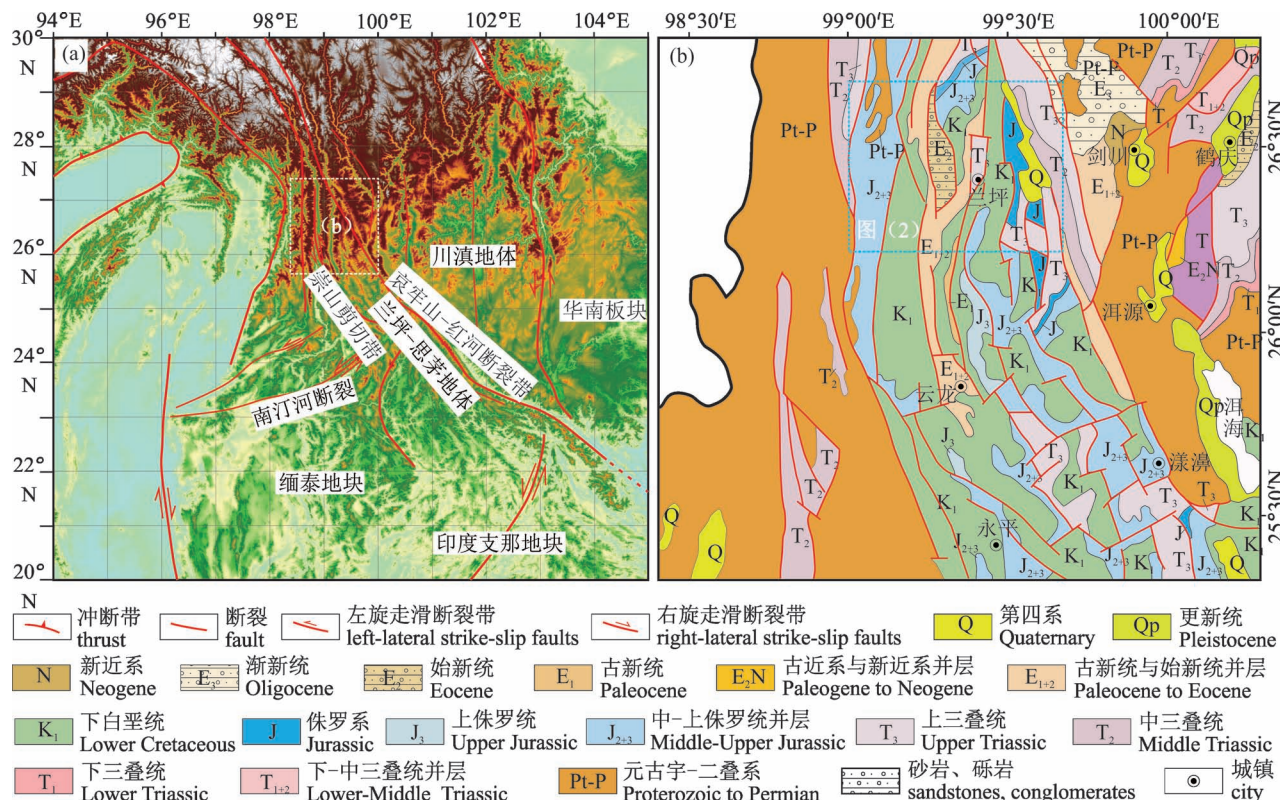


图1 青藏高原东南缘地质构造简图(a)及兰坪—思茅地体北部地质简图(b)

Fig. 1 (a) Simplified geological map of the southeastern edge of Xizang (Tibetan) Plateau; (b) simplified geological map of the northern part of the Lanping—Simao terrane

了其与川滇地体的构造边界(Wang and Burchfiel, 2000; 图1)。同位素热年代学和构造地质学研究表明,金沙江—哀牢山—红河走滑断裂带在32~17 Ma之间经历了左旋走滑运动(Leloup et al., 1995, 2001; Wang Jianghai et al., 2001; Gilley et al., 2003; Searle, 2006),自约5 Ma转化为右旋走滑运动(Gilley et al., 2003);崇山韧性剪切带自早渐新世开始了左旋走滑运动(Wang Yuejun et al., 2006; Akciz et al., 2008),Zhang Bo等(2010)则认为在崇山断裂中南段表现为左旋剪切,而在北段则表现为右旋剪切。自早古新世印度板块与欧亚大陆发生初始碰撞以来,印度板块持续的北向挤压导致兰坪—思茅地体内部广泛分布的白垩系和古近系经历了强烈的褶皱变形,从而形成了一系列褶皱轴近NW—SE向展布的逆冲推覆构造,以及NE—SW向展布的走滑断层(云南省地质矿产局, 1990; Wang and Burchfiel, 2000)。

兰坪盆地位于兰坪—思茅地体的北部,盆地内零星出露晚古生代海相—滨海相沉积地层,缺失下三叠统,广泛发育中—上三叠统至始新统碎屑沉积

(云南省地质矿产局, 1990)。盆地内部中—上三叠统属于海陆交互沉积,以灰岩和碎屑沉积为主,其与下伏上古生界呈角度不整合接触。自侏罗纪开始,兰坪盆地及周缘地区开始发育陆相碎屑沉积,白垩系自下而上划分为下白垩统景星组(浅色砂岩)、曼岗组(紫红色含长石石英砂岩)、虎头寺组(灰黄色长石石英砂岩),缺失上白垩统。古新统与下伏虎头寺组呈假整合接触。自下而上,古新统划分为下—中古新统勐野井组(棕红色泥质粉砂岩)、上古新统云龙组(紫红色粉砂岩和钙质泥岩)。始新统与下古新统云龙组整合接触。自下而上分,始新统划分为下—中始新统果郎组(钙质粉砂岩和泥岩)、上始新统宝相寺组(紫红色砂岩和黄白色石英长石砂岩)和金丝厂组(紫红色砾岩、粉砂岩、泥岩等)(云南省地质矿产局, 1990)。地层接触关系显示该区白垩系和古近系在晚始新世—中新世经历了强烈的挤压作用并形成了一系列褶皱轴近NW向展布的逆冲推覆构造(云南省地质矿产局, 1990; Sato et al., 2001; 全亚博等, 2014)。

本次研究在兰坪县以西311省道沿途的始新统

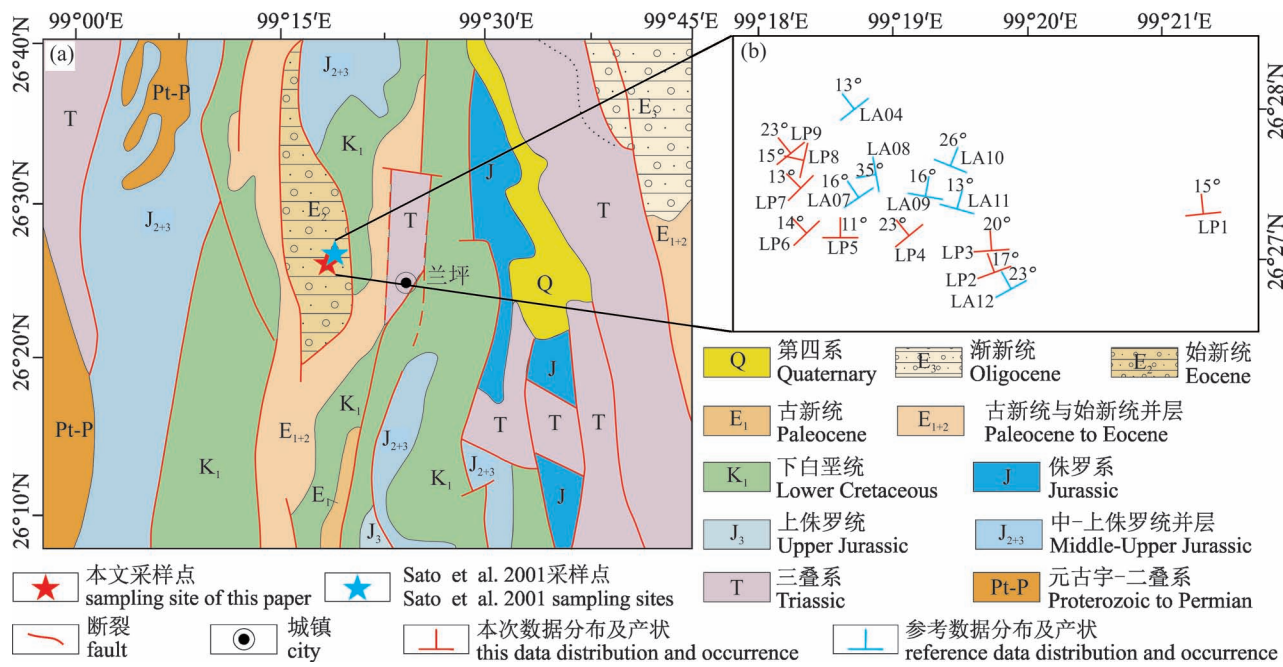


图 2 兰坪—思茅地体北部兰坪地区剖面地质简图(a) 及兰坪地区剖面古地磁采样位置及产状分布简图(b)

Fig. 2 (a) Simplified geological map of Lanping area in the northern part of Lanping—Simao terrane; (b) the distribution and occurrence of paleomagnetic sampling sites in Lanping area

宝相寺组中布置一条古地磁采样剖面(图 2a),共设置 9 个采点(LP1~LP9; 图 2b),每个采点采集 10~11 块古地磁定向岩芯样品,整条剖面共采集 91 块定向岩芯样品,同时每个采点在地层产状面上采集 3~4 块定向手标本用于磁倾角浅化矫正实验。前人通过兰坪盆地内古近系的沉积序列分析,指出兰坪盆地古近系沉积建造包含一个湖相至河流相的完整沉积旋回(朱志军等, 2011)。冯志强等(2012)通过层序地层学对兰坪盆地古近系宝相寺组进行分析,并识别出 4 个完整的三级层序。由于本次所采样品岩性均为紫红色长石砂岩、粉砂岩,自上而下粒度逐渐变细,通过层序对比,所采层位应为宝相寺组中上部,结合地层内所含古生物化石种类,本次采样地层年代应为晚始新世(Sato et al., 2001)。所有采点位置均由 GPS 定位,并使用 2015 年国际参考地磁场(International Association of Geomagnetism and Aeronomy)对采样点的现代地磁偏角进行矫正(Thébault et al., 2015)。岩芯样品均用手提式便携汽油钻机钻取,用磁罗盘定向,室内用双刀切割机将样品加工成直径 2.54 cm、高 2.3 cm 的标准样品。

2 岩石磁学实验

为了揭示兰坪盆地晚始新世紫红色砂岩样品中

载磁矿物组合类型及对剩磁的贡献,根据采样点的分布位置及样品的岩性特征,选取三块代表样品(LP1-7:砖红色中砂岩; LP5-7:紫红色泥质粉砂岩; LP8-2:紫红色泥质细砂岩)进行岩石磁学实验。分别对三块代表样品进行等温剩磁(IRM)组分分析(Kruiver et al., 2001)及等温剩磁三轴热退磁实验(Lowrie, 1990)。其中等温剩磁获得曲线由脉冲磁力仪对样品固定方向逐步加场至 2.45 T,并用 JR6 旋转磁力仪进行测试;等温剩磁三轴热退磁曲线实验按顺序分别对样品的 Z 轴、Y 轴、X 轴施加 2.45 T、0.4 T、0.12 T 的磁场,之后进行系统热退磁(Hirt and Lowrie, 1988; Lowrie, 1990)。以上所有实验均在中国地质科学院地质力学研究所自然资源部古地磁与古构造重建重点实验室完成。

三块代表样品显示了相似的 IRM 组分分析和等温剩磁三轴热退磁实验结果(图 3)。LP1-7 的 IRM 获得曲线显示,在外加直流场强小于 1000 mT 时,样品的剩磁强度逐渐上升。当外加磁场强度达到 2.45 T 时,样品剩磁强度接近饱和状态。此时样品的剩磁强度可以分离出两个剩磁组分:组分 1 矫顽力为 93.3 mT($DP = 0.44$ mT),贡献了 15.5% 的剩磁强度;组分 2 矫顽力为 489.8 mT($DP = 0.31$ mT),贡献了 84.5% 的剩磁强度。等温剩磁的三轴

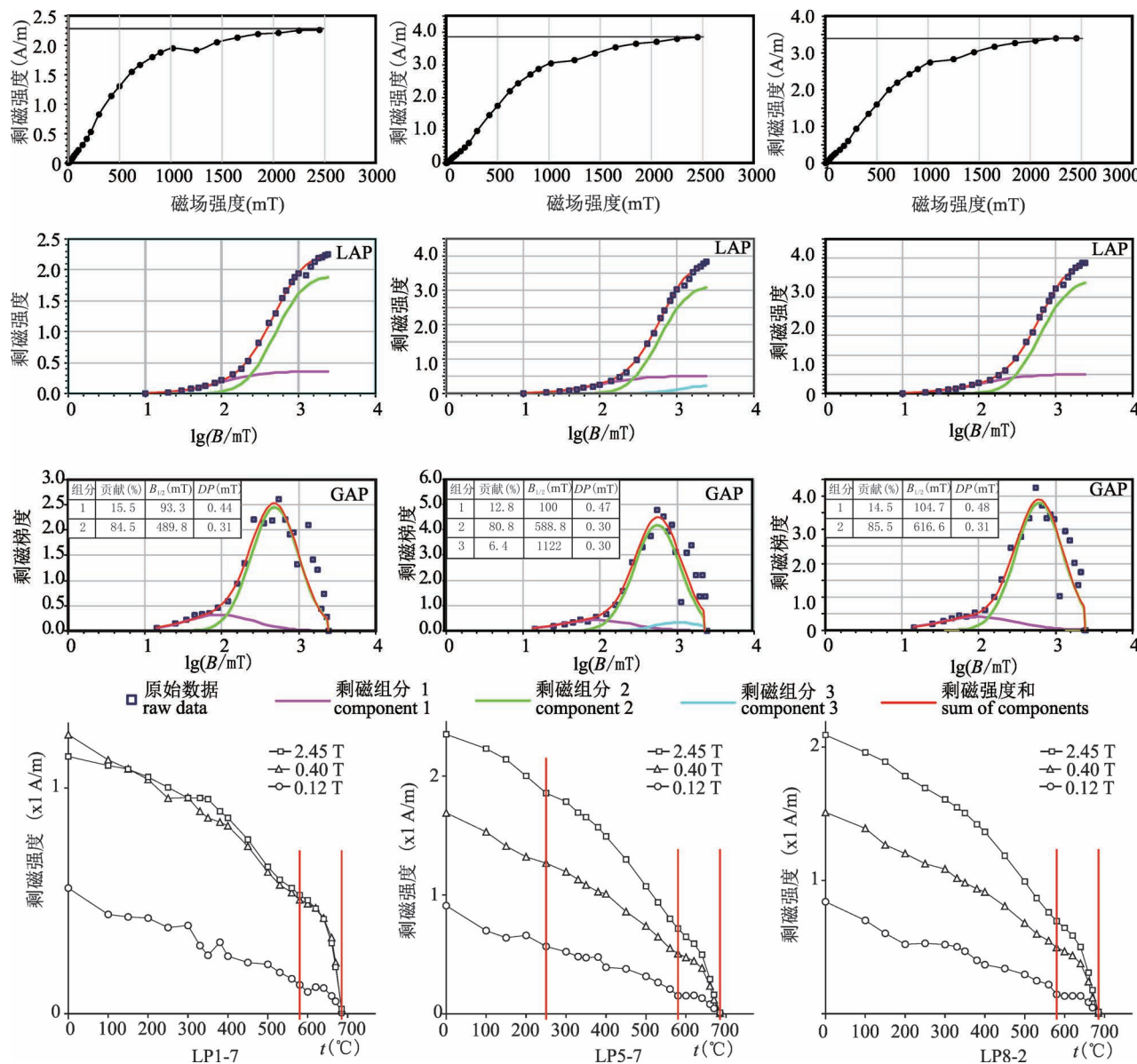


图3 代表样品岩石磁学实验结果图(从上而下依次为等温剩磁获得曲线、矫顽力谱图及等温剩磁三轴热退磁曲线)

Fig. 3 Rock magnetic results of representative specimens (Isothermal remanent magnetization acquisition curves, Coercivity spectrum and thermal demagnetization of a three-component isothermal remanent magnetization from top to bottom)

热退磁实验结果显示,样品的中、软磁组分在580℃左右出现显著的拐点,显示了磁铁矿的信息(Ozdemir and Dunlop, 1993; Butler, 1998),此外硬、中、软磁组分在640℃以后迅速下降并在685℃降为0,指示了赤铁矿的解阻温度(图3)。因此,组分1可能代表了磁铁矿,组分2应为赤铁矿。LP5-7和LP8-2的IRM获得曲线基本一致,在外加直流场强达到1000 mT之前缓慢上升,直至2.45 T仍未达到饱和。其中样品LP5-7的剩磁强度可分离出三个组分,组分1矫顽力为100 mT($DP=0.47$ mT),贡献

了12.8%的剩磁强度;组分2矫顽力为588.8 mT($DP=0.30$ mT),贡献了80.8%的剩磁强度;组分3矫顽力为1122 mT($DP=0.30$ mT),贡献6.4%的剩磁强度;LP8-2可分离出两个组分,组分1矫顽力为104.7 mT($DP=0.48$ mT),贡献了14.5%的剩磁强度;组分2矫顽力为616.6 mT($DP=0.31$ mT),贡献了85.5%的剩磁强度。三轴热退磁实验结果显示,LP5-7的硬磁组分在250℃左右微弱下降,可能是针铁矿解阻的结果,表明其组分3可能为针铁矿;此外两个样品的三个磁组分在580℃左右都出现了明显

的拐点,剩磁强度最终在 685°C 快速降低为 0(图 3),表明了磁铁矿和赤铁矿的存在。因此从 LP5-7 和 LP8-2 分离出的组分 1 和组分 2 应当分别为磁铁矿和赤铁矿。

三块代表性样品的多类别岩石磁学实验结果表明,本次研究在兰坪盆地始新世红层中采集的构造磁学岩心样品的载磁矿物组合主要为磁铁矿和赤铁矿,另含有少量的针铁矿。

3 系统热退磁结果

根据岩石磁学实验结果,对所有的始新世红层样品进行了系统热退磁实验。系统热退磁使用英制 TD-48 大型热退磁炉完成,低温段温度间隔为 50~100°C,当热退磁温度超过 500°C 后,热退磁段温度间隔减小至 20~30°C。样品的剩磁方向测量使用美制 2G-755 型超导磁力计,样品的热退磁曲线以正交矢量投影方式展示(Zijderveld, 1967),特征剩磁分量使用主向量分析法或者重磁化大圆弧交汇法分离获得(Kirschvink, 1980; Halls, 1976, 1978)。以

样品为单位对获得的剩磁分量进行 Fisher 统计(Fisher, 1953),得到采点的平均剩磁方向,之后以采点为单位进行 Fisher 统计(Fisher, 1953),获得研究剖面的平均剩磁方向(表 1)。

在热退磁温度区间 0~300°C 内,可以从 37 块地始新世红层样品中分离出低温剩磁分量(图 4)。以样品为单位对低温剩磁分量进行 Fisher 统计,获得低温剩磁分量的平均方向为:在地层矫正前低温剩磁分量的平均方向为: $D_g = 345.8^\circ, I_g = 48.7^\circ, k = 20.8, \alpha_{95} = 5.3^\circ, n = 37$;地层矫正后的平均方向为: $D_s = 345.5^\circ, I_s = 36.0^\circ, k = 17.3, \alpha_{95} = 5.8^\circ, n = 37$ (图 5a)。地层矫正后的精确参数 k 微弱减小(由 20.8 变为 17.3),而 α_{95} 增大(由 5.3° 到 5.8°),虽然矫正前的低温剩磁分量的磁倾角与现代地球磁场方向($D = 4.0^\circ, I = 43.9^\circ$)和地球偶极子场期望值($D = 0^\circ, I = 44.8^\circ$)相近,但磁偏角与现在地磁场相差近 20°,这可能与可分离出低温分量的样品过少,导致统计结果存在较大的误差有关。因此可以推测低温剩磁分量为现代地磁场下形成的粘滞剩磁。

表 1 兰坪地区剖面晚始新世高温剩磁分量

Table 1 High temperature magnetic components of late Eocene from the Lanping area

采点	位置 N/E(°)	产状 S/D(°)	年 代	n/N	矫正前		矫正后		K_s	α_{95s}	古地磁极		A_{95}
					Dec. (°)	Inc. (°)	Dec. (°)	Inc. (°)			Lat. (°N)	Lon. (°E)	
本次研究所采剖面													
LP1	26°27'12"/99°21'03"	264/15	E ₂	9/10	75	39.1	63.9	35.3	85.4	5.6	31.3	181.7	4.9
LP2	26°27'09"/99°19'44"	250/20	E ₂	4/9	290	-29.9	278	-41.2	94.5	12.9	3.7	164.7	12.3
LP3#	26°27'12"/99°19'43"	266/17	E ₂	0/10	-	-	-	-	-	-	-	-	-
LP4	26°27'21"/99°19'03"	302/23	E ₂	7/11	278.8	-52.7	258.4	-39.7	11.4	16.2	19.7	173.3	15.1
LP5	26°27'23"/99°18'32"	270/11	E ₂	10/10	250.8	-47.5	240.7	-43	29.7	12.9	35.8	176.4	12.6
LP6	26°27'22"/99°18'17"	226/14	E ₂	10/11	291.4	-15.1	288.7	-28.3	12.9	14.6	9.3	347.2	11.9
LP7#	26°27'40"/99°18'16"	225/13	E ₂	7/9	284.9	41.7	289.4	30.3	129.3	6.5	24.2	16.2	5.4
LP8	26°27'58"/99°18'17"	191/15	E ₂	11/12	271.9	-25.6	271.5	-30.5	12.9	14.1	5.9	173.9	11.7
LP9#	26°27'54"/99°18'11"	231/23	E ₂	0/9	-	-	-	-	-	-	-	-	-
Sato 等 2001 所采剖面													
LA04	26°28'12"/99°18'36"	232/13	E ₂	6/8	285.3	-8.7	283.3	-19.1	63.0	8.6	7.3	354.5	6.5
LA07	26°27'36"/99°18'36"	236/16	E ₂	5/8	279.3	-20.0	273.5	-30.5	31.5	13.8	4.2	173.1	11.5
LA08	26°27'36"/99°18'36"	170/35	E ₂	4/8	254.8	-27.7	250.4	-62.5	37.4	15.2	31.7	152.3	21.0
LA09#	26°27'36"/99°19'12"	280/16	E ₂	4/8	275.6	-51.6	257.7	-47.8	17.1	22.9	22.5	167.1	24.1
LA10	26°27'36"/99°19'12"	292/26	E ₂	7/8	293.5	-57.3	258.8	-49.5	24.4	12.5	22	165.3	13.5
LA11	26°27'36"/99°19'12"	285/13	E ₂	6/8	282.1	-38.7	272.0	-37.0	19.4	15.6	7.3	169.9	14.0
LA12	26°27'00"/99°19'48"	242/23	E ₂	8/9	256.6	-39.8	236.5	-41.5	11.1	17.4	39.2	179.1	16.0
本次研究剖面高温剩磁分量平均方向					274.3	-36.0	264.2	-37.6	24.3	13.9	14.2	172.6	12.6
本次研究和 Sato 等(2001)两个剖面综合高温分量平均方向					274.5	-34.4	264.5	-39.4	21.4	9.6	14.4	171.2	8.9

注:褶皱检验(McFadden, 1990):地层矫正前 ζ_1 (IS) = 6.562, 地层矫正后 ζ_1 (TC) = 1.236, 在 95% 和 99% 的置信度下的临界值分别为 $\zeta_c = 4.036, \zeta_c = 5.624$, 在 95% 和 99% 的置信度下通过褶皱检验。褶皱检验(Watson and Enkin, 1993): $DC_{slope} = 0.731 \pm 0.553$, 在 95% 的置信度下通过褶皱检验。S/D—采样地层走向和倾角; n/N—分别为每个采点采样数量和用于 Fisher 统计的样品数。Dec.—磁偏角; Inc.—磁倾角; K_s —地层矫正后结果的精确参数; Lat./Lon.—古地磁极纬度和经度; α_{95s}/A_{95} —95% 置信区间。#代表该采点没有参与数据统计。

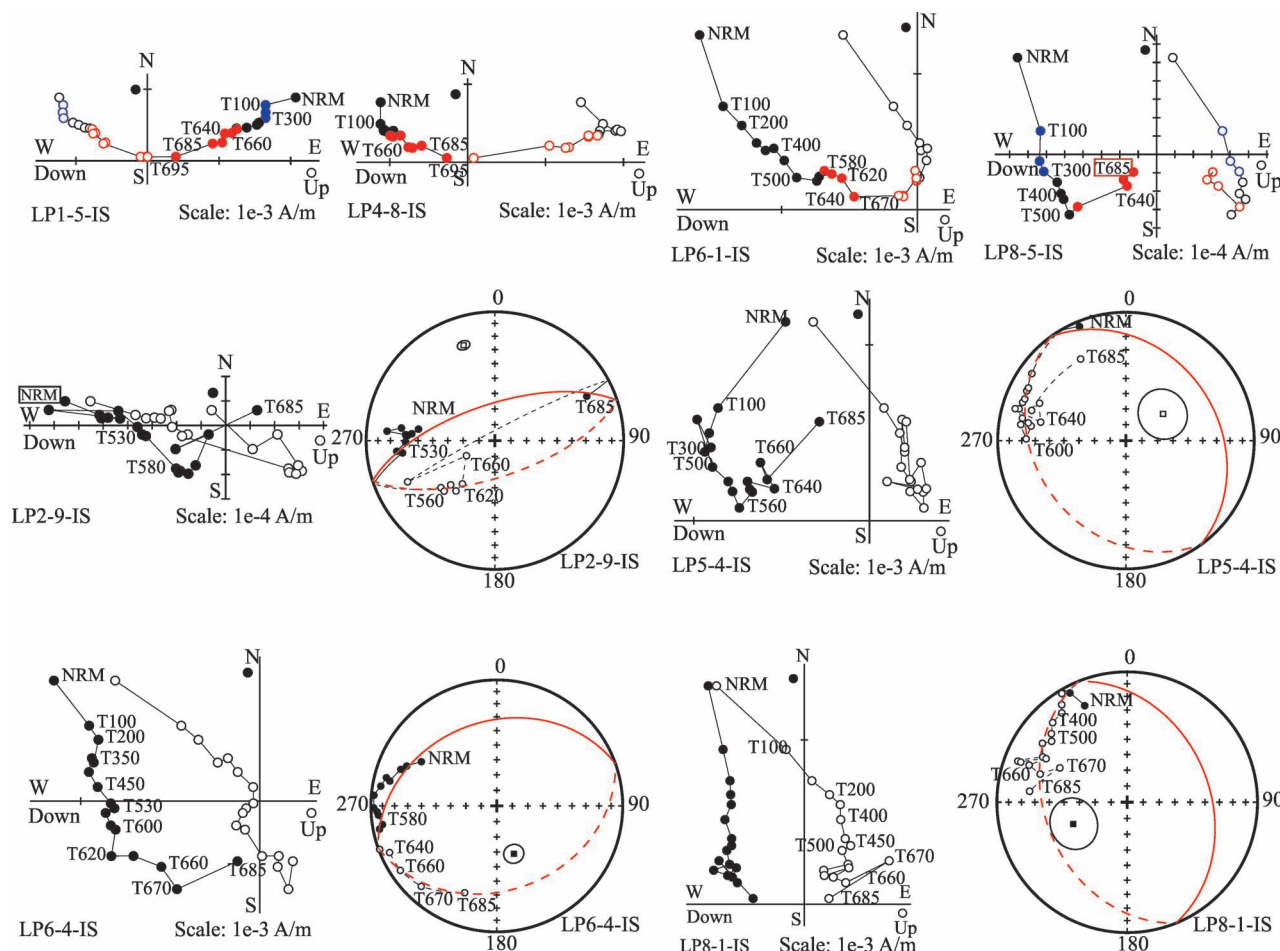


图4 兰坪地区剖面代表性样品系统热退磁结果正交矢量投影图和等面积投影图(地层矫正前);正交矢量投影图中实心圆和空心圆分别代表退磁过程中剩磁分量在水平方向和垂直方向的投影,蓝色和红色圆分别代表拟合低温分量和高温分量所用退磁步骤,等面积投影图中实心圆和空心圆分别代表正、反极性投影

Fig. 4 Orthogonal projections and Equal-area projections of magnetization vector end-points for representative specimens from the Lanping, in geographic coordinates. Solid and open circles of Orthogonal projections represent projections in the vertical and horizontal planes, respectively. The blue points and red points respectively represent projections of the demagnetization temperature intervals of the low-temperature magnetic component and high-temperature magnetic component. Solid and open circles of Equal-area projections represent the lower and upper hemispheres, respectively

绝大多数样品在300~685℃都分离出了高温剩磁分量。由于LP3, LP7和LP9三个采点样品的热退磁曲线混乱,且未展现出重磁化大圆弧退磁形态,因此无法分离出可靠的高温剩磁分量。LP1, LP2, LP4~LP6以及LP8六个采点中约2/5的样品的退磁曲线在300~685℃之间表现出很好的线性归零趋势,故用主向量分析法分离获得高温剩磁分量,其余约3/5样品的高温剩磁分量使用重磁化大圆弧交会法获得(图4)。以采点为单位对高温剩磁分量进行Fisher统计,结果表明,地层矫正前的高温剩磁分量平均方向为: $D_g = 274.3^\circ, I_g = -36.0^\circ, k = 16.9, \alpha_{95} = 16.8^\circ, N = 6$ 个采点;地层矫正后高温剩磁的平均

方向为: $D_s = 264.2^\circ, I_s = -37.6^\circ, k = 24.3, \alpha_{95} = 13.9^\circ, N = 6$ 个采点(图5b)。Sato等(2001)也曾在兰坪县以西区域($26^{\circ}28'12''/98^{\circ}18'54''$)上始新统宝相寺组红层中采集了9个采点(共计84块定向岩芯样品)开展构造磁学研究(LA04~LA12),并获得古地磁数据(LA04及LA07~LA12,共7个采点)(图2b),我们的结果与Sato等(2001)进行对比,两者在95%水平上无显著差异。但是由于LA09采点数据 α_{95} 数值偏大($\alpha_{95} = 22.9^\circ$),因此在对现有数据进行综合分析时没有采用该采点数据。结果显示地层矫正前的兰坪盆地始新世红层高温剩磁分量为 $D_g = 274.5^\circ, I_g = -34.4^\circ, k = 17.2, \alpha_{95} = 10.8^\circ, N = 12$ 个

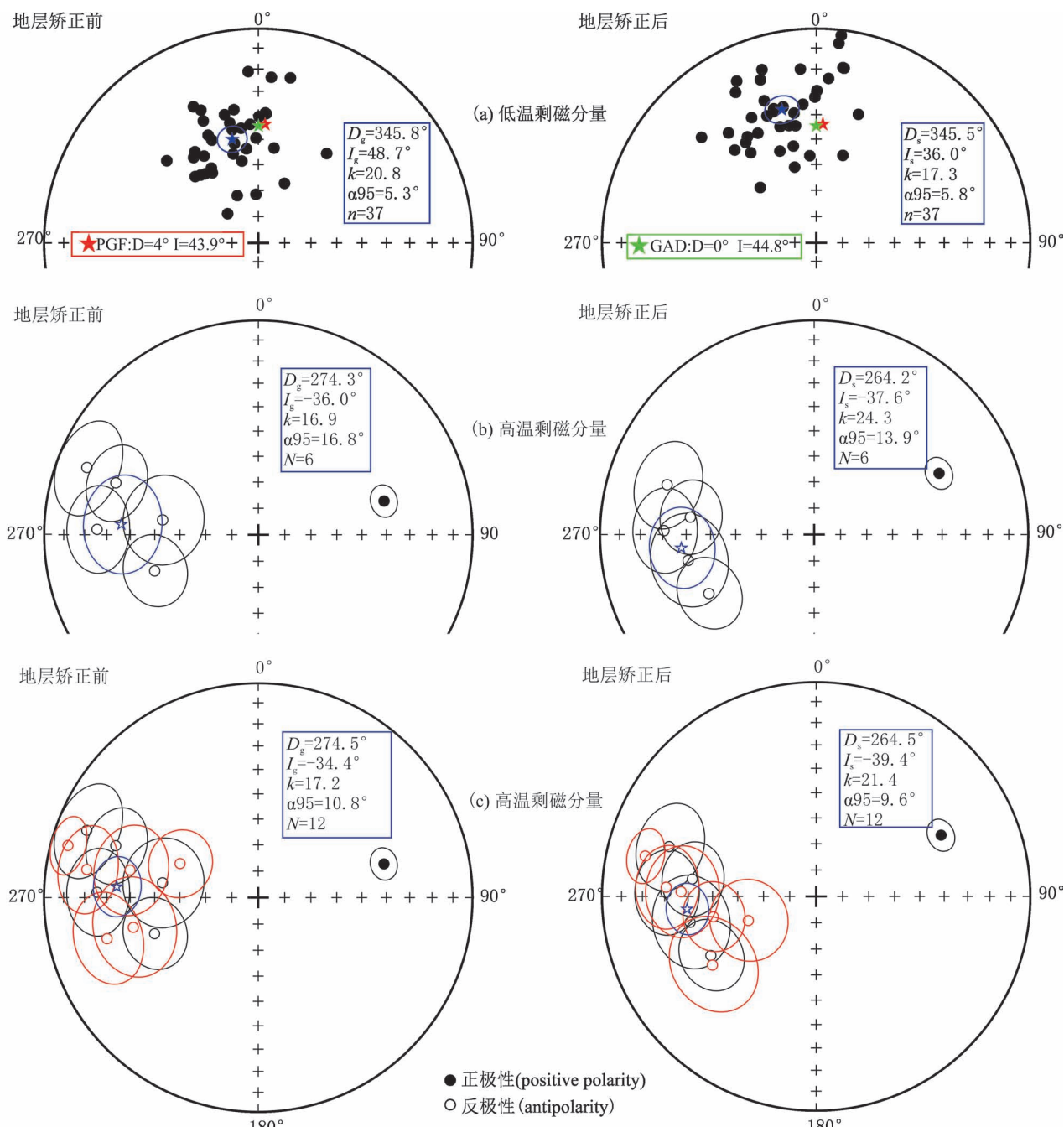


图 5 兰坪地区剖面剩磁分量等面积投影图 ; (a) 低温剩磁分量; (b) 高温剩磁分量; (c) 本次所采剖面与 Sato 等 (2001) 所采剖面高温剩磁分量等面积投影图

Fig. 5 Equal-area projections of themagnetic component from the Lanping; (a) Equal-area projections of the low-temperature component for each samplefrom the Lanping. (b) Equal-area projections of the high-temperature component for each sitefrom the Lanping. (c) Equal-area projections of the high-temperature component for each site of this study and Sato et al. 2001

红色符号代表 Sato 等 (2001) 高温数据; 蓝色五角星代表高温分量平均方向; 红色五角星 (PGF) 和绿色五角星 (GAD) 分别代表现代地球磁场方向和地球偶极子场模型期望值

The red data points are cited from Sato et al. 2001. PGF—Present Geomagnetic Field; GAD—Geomagnetic Axial Dipole Field

采点; 地层矫正后高温剩磁的平均方向为: $D_s = 264.5^\circ, I_s = -39.4^\circ, k = 21.4, \alpha_{95} = 9.6^\circ, n = 12$ 个采点 (图 5c)。由于两条剖面中获得的高温剩磁分量

只有一个采点显示为正极性, 所以无法进行正反极性倒转检验, 但该高温剩磁分量的褶皱检验 (McFadden, 1990) 显示: 地层矫正前 ζ_1 (IS) =

表2 兰坪—思茅地体北部和中部白垩纪及古近纪古地磁数据
Table 2 The Cretaceous and Paleogene paleomagnetic data obtained from the northern and central parts of the Lanping–Simao terrane

研究区	剖面位置 (°N/E)	年代	采点	实测结果				期望古纬度(°N)	实测古纬度(°N)	旋转量(°)	Sa	$Sa-Sa'$ (°) $Sr=149°$	参考文献		
				Dec.(°)	Inc.(°)	α_{95}	Lat.(°N)								
兰坪	26.5/99.3	E ₂	12	264.5	-39.4	9.6	14.4	171.2	8.9	19.4	22.4	-3.0±6.9	80.3±8.9	-49	C
兰坪	26.5/99.3	E ₂	9	86.1	39.8	11.2	13.2	170.4	10.4	19.4	22.6	-3.2±9.2	81.8±9.9	-49	C
云龙	25.8/99.4	K ₂	20	40.2	49.9	3.9	54.4	172.0	4.3	20.5	30.7	-10.5±3.4	29.8±3.9	5	B
云龙	25.8/99.4	K ₂	29	38.3	50.7	3.4	56.1	170.8	3.8	20.5	31.4	-11.0±3.1	27.8±3.6	5	B
永平	25.5/99.5	K ₁	12	42.0	51.1	15.7	52.8	169.8	17.5	23.9	31.8	-8.1±12.9	32.2±15.2	6	A
下关	25.6/100.2	K ₂	9	6.9	47.7	8.6	83.1	161.2	9.0	20.4	28.8	-8.4±6.8	3.6±7.7	2	B
巍山	25.3/100.4	K ₂	18	64.3	48.5	4.7	33.5	170.5	5.0	20.1	29.5	-9.4±3.8	53.7±4.4	-23	B
景东	24.5/100.8	K ₁₊₂	13	8.3	48.8	7.7	81.0	153.7	8.2	21.5	29.7	-8.2±6.1	1.9±7.1	14	D
镇沅	24.2/101.0	K ₁₊₂	7	61.8	46.1	8.1	34.9	173.4	8.3	21.3	27.5	-6.2±6.2	51.6±7.0	-39	D
A	K ₁ (145.5~99.6 Ma) K ₂ (99.6~65.5 Ma)				纬度=80.9 纬度=79.0 纬度=81.9 纬度=80.2				经度=197.4 经度=216.2 经度=249.6 经度=206.3				$A_{95}=1.5$ $A_{95}=1.8$ $A_{95}=6.9$ $A_{95}=1.7$	N=4 N=3 N=2 N=7	选自 Cogné et al., 2013 建立的视极移曲线
B	K ₂ (99.6~65.5 Ma)														
C	E(55.8~33.9 Ma)														
D	K ₁ +K ₂ (145.5~65.5 Ma)														

注: F₂—始新世; K₁—早白垩世; K₂—晚白垩世; Dec./Inc.—磁偏角和磁倾角; Lat./Lon.—古地磁极的纬度和经度; α_{95}/A_{95} —95%置信区间; Sa—不同古地磁研究区构造线迹展布方向; Sr—原生参考线迹方向; Sr-Sa—构造线迹变化量。

6.562, 地层矫正后 $\zeta_1(\text{TC}) = 1.236$, 在 95% 和 99% 的置信度下的临界值分别为 $\zeta_c = 4.036$ 、 $\zeta_c = 5.624$, 表明在 95% 和 99% 的置信度下通过了 McFadden (1990) 的褶皱检验。此外, 高温剩磁分量还在 95% 的置信度下通过了 Watson 和 Enkin (1993) 的褶皱检验 ($DC_{\text{slope}} = 0.731 \pm 0.553$)。通过该区地层接触关系的研究, 兰坪地区发生褶皱的年代为晚始新世—中新世时期, 正褶皱检验结果则表明该高温分量为褶皱前获得。因此, 本次研究从晚始新世宝相寺组红层中分离出的高温剩磁分量应是地层沉积成岩过程中形成的原生特征剩磁分量。

4 讨论

4.1 兰坪—思茅地体北部兰坪盆地的新生代地壳旋转变形特征

古近纪以来, 由于印度板块持续挤压欧亚大陆, 导致青藏高原东南缘地壳物质发生了东南侧向挤出逃逸运动, 其间伴随着大角度顺时针旋转运动 (Funahara et al., 1992; Yang Zhenyu and Besse, 1993; Huang Kainian and Opdyke, 1993; 杨振宇等, 1998; Sato et al., 1999, 2007; Tappognier et al., 2001; Otofuji et al., 2012; Tong Yabo et al., 2013, 2015, 2016; Wang Heng et al., 2016; Li Shihu et al., 2017)。在针对东亚白垩纪和新生代地壳运动和构造变形的构造磁学研究中, 选取 Cogné 等 (2013) 建立的东亚大陆白垩纪和新生代视极移曲线为参考古地磁极, 来定量约束地壳的运动方式和幅度。以东亚地区 55.8~33.9 Ma 的古地磁极 ($81.9^{\circ}\text{N}, 249.6^{\circ}\text{E}, A_{95} = 6.9^{\circ}$) 作为参考极, 计算得出兰坪盆地的期望磁偏角和磁倾角分别为: $D_e = 4.2^{\circ}, I_e = 35.1^{\circ}, \alpha_{95} = 6.5^{\circ}$, 期望古纬度为 $\lambda = 19.4^{\circ}\text{N}$ 。这表明兰坪—思茅地体北部的兰坪盆地自晚始新世以来相对于东亚稳定参考极发生了 $80.3 \pm 8.9^{\circ}$ 的顺时针旋转运动。然而, 前人在兰坪盆地以南的云龙、永平、下关等地区白垩纪和古近纪地层中获得的古地磁数据表明, 这些地区相对于东亚古地磁极仅经历了不超过 30° 的顺时针旋转运动 (Sato et al., 1999; Funahara et al., 1993; Huang Kainian and Opdyke, 1993; Yang Zhenyu et al., 2001; Tanaka et al., 2008) (图 6a, 表 2), 明显小于兰坪地区约 80° 的顺时针旋转量。这些从兰坪—思茅地体北部和中部地区获得的白垩纪和古近纪古地磁数据表明, 兰坪—思茅地体中部和北部区域发生了显著的差异性旋转变形。前人研究认为地体中部的差异性旋转变形与地

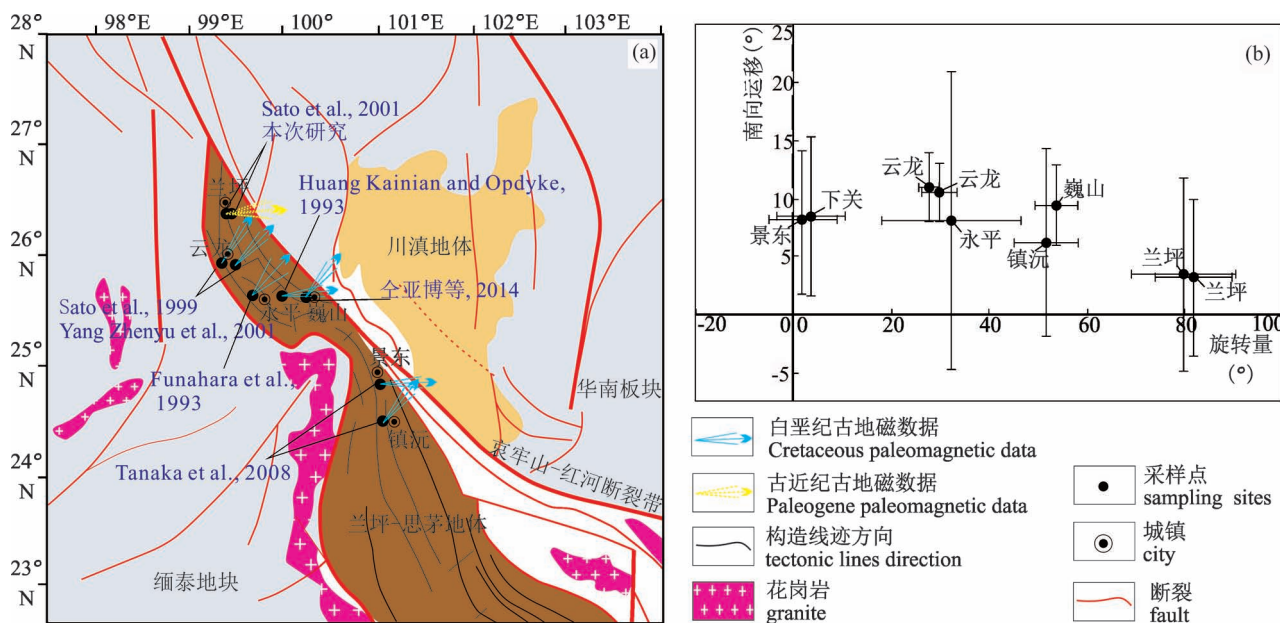


图 6 (a) 兰坪—思茅地体不同研究区旋转量变化图(修改自 Tong Yabo et al. , 2013);
 (b) 兰坪—思茅地体不同研究区旋转量与南向运移量的关系图

Fig. 6 (a) Variation of rotation in different study areas of Lanping—Simao terrane (modified from Tong Yabo et al. , 2013);
 (b) Relationship between rotation and southward displacement in different study areas of Lanping Simao terrane

壳变形所致的弧形构造线迹相关(全亚博等, 2014; 徐颖超等, 2017)。为了剖析兰坪—思茅地体北部和中部差异性旋转变形的成因及动力机制, 本次研究采用线性回归分析法来解析兰坪—思茅地体内部旋转变形与构造线迹的相关性(Voo and Channell, 1980; Schwartz and Voo, 1983, 1984)。兰坪—思茅地体内部白垩系和古近系褶皱和断层发育, 构成了一系列线性构造线迹。以金沙江—哀牢山—红河走滑断裂带北段构造线迹方向作为北部和中部研究区的原生构造线迹参考方向($Sr = 149^\circ$), 计算出兰坪—思茅地体北部和中部不同构造磁学研究区由褶皱轴和逆冲断层所组成的构造线迹(Sa)相对于原生构造线迹的变化量($Sr-Sa$)。之后对各区的构造线迹变化量($Sr-Sa$)与对应的旋转量进行最佳线性拟合(图 7)。拟合结果显示线性相关系数 $R = 0.96$, 表明兰坪—思茅地体北部和中部的旋转变形量与构造线迹变化量成线性相关。因此, 研究区内的差异性旋转运动与构造线迹展布方向的变化同步, 且有着共同的动力机制, 即地壳构造变形导致了局部差异性旋转运动。将研究区内现今构造线迹还原为原生线迹参考方向时, 兰坪—思茅地体北部和中部的旋转运动量统一矫正为约 20° , 表明在发生差异性旋转变形前, 兰坪—思茅地体北部和中部地

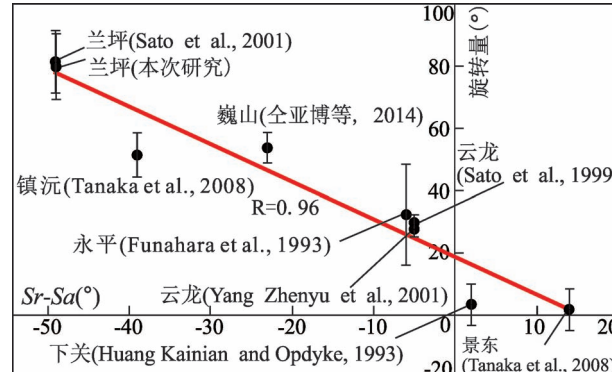


图 7 兰坪—思茅地体北部和中部不同古地磁研究区构造线迹变化量与旋转量关系图; Sr —原生参考线迹方向; Sa —不同古地磁研究区构造线迹展布方向; $Sr-Sa$ —构造线迹变化量; R —线性相关系数; 红线为最佳拟合线
 Fig. 7 The correlation of the variation of tectonic lines and the rotation in different paleomagnetic study areas in the northern and central part of Lanping—Simao terrane. Sr —the strikes of reference tectonic lines; Sa —the arithmetic average strikes of tectonic lines in different paleomagnetic study areas; $Sr - Sa$ —tectonic lines variation; R —the correlation coefficient; the red line is the best-fit linear regression

区经历了约 20° 的整体顺时针旋转运动。Tong 等(2013)对勐腊地区白垩系和始新统红层进行的详

细构造磁学研究,表明思茅地体自早渐新世以来,经历了约37°的顺时针旋转挤出运动,其中在35~17 Ma受印亚碰撞及持续的北向挤压作用下,与印支地块南部共同经历约22°的整体顺时针旋转挤出运动,而后又进一步经历约15°的局部顺时针旋转变形(Tong Yabo et al., 2013; 全亚博等, 2014)。这与本次研究从兰坪—思茅地体北部中部分离出的地体整体性顺时针旋转变形量相吻合。自印亚碰撞以来,受印度板块持续向北及逆时针旋转运动的影响,特提斯—喜马拉雅地体东部沿雅鲁藏布缝合带北向楔入欧亚大陆内部,并逐渐形成东喜马拉雅构造节(刘宇平等, 2000)。最新的热年代学和构造地质学研究认为,虽然实皆右旋走滑断裂带作为西缅甸地块和缅泰地块间的构造边界,自约28~27 Ma以来开始了右旋走滑活动,并累积了约400 km的右旋错断量,但是其右旋走滑运动并非完全受控制于缅泰地块的南向挤出逃逸运动,而主要与西缅甸地块的大规模北向运动相关(Maurin and Rangin, 2009; Licht et al., 2018; Morley and Arboit, 2019)。因此,在印度板块东端和西缅甸地块强烈的北向挤压共同作用下,东喜马拉雅构造节发生大规模的北北东向运移(约500 km),逐渐形成拇指状构造结(王二七等, 2001; 张进江等, 2001)。在这一过程中,青藏高原东南缘在渐新世以来势必会遭受强烈的挤压和地壳缩短变形(Burg et al., 1998; Zeitler et al., 2001),从而导致紧邻东喜马拉雅构造节的区域在地壳侧向顺时针旋转挤出逃逸过程中进一步遭受局部的顺时针旋转变形,使得兰坪地区在整体20°顺时针旋转运动的基础上又叠加了近60°(与本区构造线迹变化量基本一致)的局部地壳顺时针旋转变形,而南部云龙、永平等地则叠加极少的局部顺时针旋转变形,从而保持30°以内的顺时针旋转量,并最终造成兰坪盆地经历高于南部地区的顺时针旋转变形。前人研究表明,哀牢山—红河断裂于32~17 Ma发生左旋走滑运动(Leloup et al., 1995, 2001; Wang Jianghai et al., 2001; Gilley et al., 2003; Searle, 2006),并于约5 Ma转化为右旋走滑运动(Gilley et al., 2003);而鲜水河—小江断裂带在中新世至早新世(约17~5 Ma)开始发生初始的左旋走滑运动(Roger et al., 1995; Wang Shifeng et al., 2009; Li Shihu et al., 2015),此时川滇地体开始沿鲜水河—小江断裂带发生顺时针旋转挤出运动,这一过程中,势必导致川滇地体对兰坪—思茅地体强烈的南向挤压。受印亚碰撞影响,渐新

世以来(37~21 Ma),兰坪—思茅地体南缘的临沧—勐连花岗岩经历了由南向北的逐步隆升(施小斌等, 2006)。在印支地块大规模南向挤出过程中,兰坪—思茅地体中部区域受临沧—勐连花岗岩带的阻挡而导致地体中部的强烈地壳构造变形,形成了北向凸出的蜂腰状构造形态。在这一过程中,兰坪—思茅地体蜂腰部位及以北的景东、五印、下关等地经历较小的顺时针旋转(10°以内)变形(Huang Kainian and opdyke, 1993; 全亚博等, 2014),而以南景谷、普洱等地在上新世以来川滇地体挤压综合作用下则发生50°~70°的顺时针旋转变形(Huang Kainian and opdyke, 1993; Chen Haihong et al., 1995; Sato et al., 2007)。因此兰坪—思茅地体中部蜂腰处强烈的差异性顺时针旋转变形可能与地壳构造变形相关(Kondo et al., 2012; Tong Yabo et al., 2013; Gao Liang et al., 2015; 徐颖超等, 2017)。

兰坪—思茅地体北部的兰坪盆地,以及保山地体和腾冲地体自早渐新世以来发生的高达约80°的顺时针运动是地块整体顺时针旋转挤出逃逸和局部地壳顺时针旋转变形作用叠加的结果,而中部强烈的差异性顺时针旋转变形则与川滇地块南向挤压和临沧花岗岩带的阻挡相关。这表明,青藏高原东南缘地壳块体在新生代普遍经历了与地壳构造变形相关的局部差异性旋转变形作用,并非表现为刚性块体性质。

4.2 印支地块北部兰坪—思茅地体南向差异性运移的原因及其构造意义

古地磁研究结果表明兰坪—思茅地体中南部自印度板块与欧亚大陆碰撞以来沿着哀牢山—红河走滑断裂带经历了400~700 km的纬向运移(Yang Zhenyu and Besse, 1993; Sato et al., 1999; Yang Zhenyu et al., 2001; Replumaz and Tapponnier, 2003; Tanaka et al., 2008; Otofuji et al., 2012; 李仕虎等, 2012; 张海峰等, 2012; 全亚博等, 2014; 安纯志等, 2017),这与野外地质调查所估算出的哀牢山—红河断裂带左旋走滑量相吻合(Tapponnier et al., 1982; Lee and Lawver, 1995; Leloup et al., 1995; Chung Sunlin et al., 1997; Royden et al., 2008)。但是,兰坪—思茅地体北部的兰坪盆地,中部的云龙和永平等地的古地磁结果却显示出了差异性的纬向运动(Funahara et al., 1993; Huang Kainian and Opdyke, 1993; Sato et al., 1999, 2001; Yang Zhenyu et al., 2001; 全亚博等, 2014)。本次

研究及 Sato 等(2001)从兰坪盆地始新世地层中获得的古地磁数据表明,自晚始新世以来兰坪地区相对东亚稳定参考极发生了 $3.0^{\circ}\pm6.9^{\circ}$ 的不显著南向运移量,而南部的云龙、永平、巍山、下关等地则发生了 $6^{\circ}\sim10^{\circ}$ 的南向运动(Sato et al., 1999; Tanaka et al., 2008; Yang Zhenyu et al., 2001; 全亚博等, 2014)。兰坪—思茅地体内部不同古地磁研究剖面纬度位置与其计算出地壳运动之间的对应变化趋势表明(图 6b, 表 2),兰坪—思茅地体最北部在新生代经历的顺时针旋转量最大,但南向运移量最小,而兰坪—思茅地体中部地区经历的顺时针旋转较小,但南向运移量最大,这种变形趋势似乎表明兰坪—思茅地体的上地壳是在下地壳通道流的驱动下发生了韧性变形。如果兰坪—思茅地体北部和中部地区之间存在如此大的纬向运动差异,其势必会导致地体北部和中部地区经历强烈的近南东—北西向的伸展作用,从而形成一系列地堑和近北东—南西向展布的正断层。然而,兰坪—思茅地体北部主要发育一系列近北西—南东走向的逆冲断层以及近北东—南西走向的走滑断层。此外,白垩纪至古近纪地层在整个兰坪—思茅地体北部和中部地区连续出露,并不存在与伸展作用相关的地堑及正断层。因此,兰坪—思茅地体北部和中部地区始新世红层古地磁数据所显示出的差异性纬向运动,并不能代表地体北部和中部可能存在差异性南向挤出逃逸。

中亚地区中生代和新生代红层中普遍存在因沉积压实作用所导致的磁倾角偏低现象(King, 1955; Tan Xiaodong et al., 1996, 2003; Tauxe, 2005; Kodama, 2012),其会导致从红层地层中获得的磁倾角数据出现异常,从而影响纬向运移的精确估算。例如,Tong Yabo 等(2013)对兰坪—思茅地体南部勐腊地区获取的白垩纪和古近纪古地磁数据进行的磁倾角偏低矫正表明,这个地区存在显著的磁倾角浅化现象。因此,为了验证兰坪—思茅地体北部和中部的差异性纬向运动是否是由红层地层潜在的磁倾角偏低现象所引起的假象,需要对兰坪盆地内获得的始新世古地磁数据进行磁倾角偏低矫正实验。由 E/I 矫正方法(Tauxe and Kent, 2004)在对强构造变形区内产状变化较大的地层中获得的古地磁数据进行矫正时,会给出过度矫正的磁倾角,从而导致对地块纬向运动量的错误约束。因此,本次研究中采用 Hodych 和 Buchan(1994)提出的磁倾角矫正方法,对采集到的地层层面定向的块状标本进行磁倾角偏低矫正。对垂直于地层层面钻取到的岩心样

品,以 Z 轴和 X 轴组成的平面作为垂向面参考面,进行斜向 45° 加场,逐步增加直流磁场至 1000 mT。在每一步加场完毕后,使用 JR6 旋转磁力仪对样品进行剩磁测量。当完成 1000 mT 强度的加场后,对样品进行系统热退磁,并在每一步热退磁后使用 JR6 旋转磁力仪进行剩磁测量。通过公式 $\tan I_{\text{实测}}/\tan I_{\text{矫正}} = IRM_z/IRM_x = f$ (磁倾角浅化因子)来定量计算古地磁数据是否存在磁倾角偏低,以及偏低的程度,并由此对实测磁倾角进行矫正。实验结果显示(图 8, 表 3),200~1000 mT 加场过程中 $f = IRM_z/IRM_x = 0.9174$, 全程热退磁过程(200~690°C)中 $f = IRM_z/IRM_x = 0.9031$ 。由于样品中主要载磁矿物为赤铁矿和磁铁矿,且原生特征剩磁分量由赤铁矿携带,因此本次研究还计算了 600~690°C 温度区间内的 $f = IRM_z/IRM_x = 0.9151$, 结果显示 200~1000 mT 加场过程和 600~690°C 温度区间内的热退磁过程得到的 f 基本一致,这表明兰坪盆地内始新世红层经历了磁倾角浅化作用。根据 $f = 0.9151$ 对本次研究和 Sato 等(2001)获得的始新世古地磁数据平均结果进行磁倾角矫正,矫正后的原生特征剩磁分量为 $D_s = 264.5^{\circ}, I_s = -43.1^{\circ}, k = 21.4, \alpha_{95} = 9.6^{\circ}$, 表明相对东亚古地磁极,兰坪盆地自晚始新世以来发生了 $5.8^{\circ}\pm7.2^{\circ}(638\pm792 \text{ km})$ 的南向运移。虽然矫正后的数据所显示的南向位移量有所增大,但是在误差范围内仍不能确定地体北部发生了显著的南向位移。孙志明等(2001)通过对兰坪盆地东侧的雪龙山左旋韧性剪切带的中糜棱岩显微构造研究,提出其左行滑移量仅为 9.4 km。而从保山地体中获取的古地磁数据表明保山地体并没有经历显著的纬向运动(Tong Yabo et al., 2016; Li Shihu et al., 2017),如果兰坪地区发生大规模的南向运动,则会导致崇山韧性剪切带的右旋运动和雪龙山韧性剪切带的大规模左旋滑移量,这显然与地质事实不符。因此兰坪地区在新生代应当没有发生显著的纬向运动,而兰坪—思茅地体北部和中部的确存在差异性纬向运动。自印度—欧亚板块在古近纪时期初始碰撞以来,两板块间的持续近南北向挤压,以及东喜马拉雅构造带的北北东向推移,对青藏高原东南缘的腾冲地块,保山地体以及兰坪—思茅地体北部持续的施加了近北东—南西至近东西向的挤压。可以推测,东喜马拉雅构造带的形成首先给兰坪—思茅地体北部施加了近北北东—南南西向的挤压,而随着东喜马拉雅构造带地体的北北东向推进以及地体的顺时针旋转变形,兰坪—思茅地体北

表3 兰坪地区代表样品等温剩磁各向异性表

Table 3 Anisotropy of isothermal remanent magnetization for representative samples in the Lanping area

样品名	位置	样品数量	IRM_Z/IRM_X (加场)	IRM_Z/IRM_X (热退磁过程)	
			200~1000 mT	200~690°C	600~690°C
LPC1-1A	26°27'12"/99°21'03"	1	0.9218	0.9388	0.9383
LPC1-1C	26°27'12"/99°21'03"	1	0.9707	0.9760	0.9961
LPC1-1K	26°27'12"/99°21'03"	1	0.9322	0.9179	0.9400
LPC1-1M	26°27'12"/99°21'03"	1	0.9518	0.9475	0.9478
LPC1-2A	26°27'12"/99°21'03"	1	0.9303	0.9183	0.9089
LPC1-2G	26°27'12"/99°21'03"	1	0.9639	0.9658	0.9926
LPC2-1A	26°27'09"/99°19'44"	1	0.8872	0.8784	0.8856
LPC2-1D	26°27'09"/99°19'44"	1	0.9389	0.9296	0.9240
LPC2-1E	26°27'09"/99°19'44"	1	0.9296	0.8950	0.9115
LPC2-2A	26°27'09"/99°19'44"	1	0.8916	0.8629	0.8996
LPC2-2C	26°27'09"/99°19'44"	1	0.9350	0.8990	0.8944
LPC2-2D	26°27'09"/99°19'44"	1	0.8405	0.8604	0.8725
LPC4-1A	26°27'21"/99°19'03"	1	0.8663	0.8591	0.9122
LPC4-1D	26°27'21"/99°19'03"	1	0.8797	0.8643	0.8977
LPC4-1E	26°27'21"/99°19'03"	1	0.9759	0.8833	0.9472
LPC4-1F	26°27'21"/99°19'03"	1	0.9435	0.8659	0.8989
LPC4-1G	26°27'21"/99°19'03"	1	0.8435	0.8561	0.8625
LPC5-1A	26°27'23"/99°18'32"	1	0.8494	0.8897	0.8910
LPC5-2C	26°27'23"/99°18'32"	1	0.9163	0.9084	0.9277
LPC5-2F	26°27'23"/99°18'32"	1	0.9209	0.8899	0.8891
LPC5-3D	26°27'23"/99°18'32"	1	0.9263	0.8859	0.9147
LPC5-4A	26°27'23"/99°18'32"	1	0.9349	0.8959	0.9044
LPC5-5E	26°27'23"/99°18'32"	1	0.9009	0.8561	0.8919
LPC6-1A	26°27'22"/99°18'17"	1	0.9144	0.9214	0.9271
LPC6-1B	26°27'22"/99°18'17"	1	0.9898	0.9710	0.9444
LPC6-1D	26°27'22"/99°18'17"	1	0.9462	0.9525	0.9188
LPC6-2B	26°27'22"/99°18'17"	1	0.9245	0.9058	0.9230
LPC6-2C	26°27'22"/99°18'17"	1	0.8583	0.8886	0.9015
LPC6-2G	26°27'22"/99°18'17"	1	0.9095	0.9225	0.9333
LPC8-1A	26°27'58"/99°18'17"	1	0.9205	0.9010	0.8699
LPC8-1B	26°27'58"/99°18'17"	1	0.9253	0.8909	0.9008
平均值(f)		31	0.9174	0.9031	0.9151

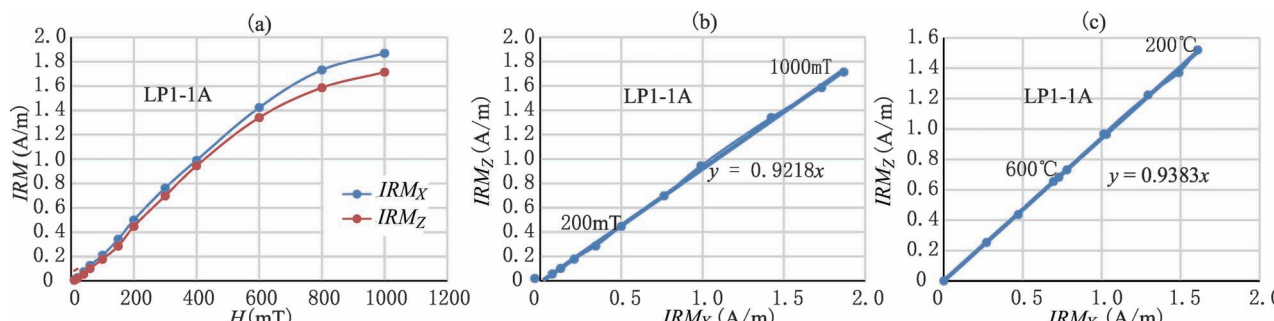
注: 兰坪地区31块代表样品校正结果; $f_{(200-1000 \text{ mT})} = 0.9174$; $f_{(200-690^\circ\text{C})} = 0.9031$, $f_{(600-690^\circ\text{C})} = 0.9151$; f 为浅化因子。

部的挤压应力逐渐转向近北东—南西向。这一应力场的变化导致兰坪—思茅地体北部始终处于垂直于地体延伸方向的挤压作用之下,从而导致该区上地

壳发生了强烈的韧性变形和横向的缩短,同时在下地壳流的驱动下向东南流出,从而形成现今的“半葫芦状”地体形态,并导致了地体北部和中部差异性的纬向运移。但是,兰坪—思茅地体中南部云龙、永平、镇沅等地地壳南向运移量基本一致且接近哀牢山—红河断裂带北段约600~700 km的左旋走滑错断量(Tappognier et al., 1982; Leloup et al., 1995; Chung Sunlin et al., 1997),表明沿大型走滑断裂带的侧向挤出逃逸模式在兰坪—思茅地体挤出逃逸过程中仍然存在。

综上所述,印支地块北部的兰坪—思茅地体中南部在始新世以来应当发生了较为整体性的东南侧向顺时针旋转挤出逃逸。但是,由于地体北部受到垂直于地体伸展方向的挤压作用,导致了上地壳的近北东—南西向缩短和北西—南东向伸展,从而造成地体北部的南向位移量小于地体中部。这种地壳运动特征表明,至少在印支地块北部地区,上地壳沿大型走滑断裂带发生的东南向挤出逃逸运动和下地壳通道流所导致的上地壳韧性变形作用共存或者在不同阶段分别有着控制作用。而地体内部经历的局部差异性地壳旋转变形作用是由于东喜马拉雅构

造节的楔入及临近块体的挤压作用导致的地壳构造变形引起。其中地体北部由于受东喜马拉雅构造节的北东—东向挤压作用,导致地壳在整体顺时针旋



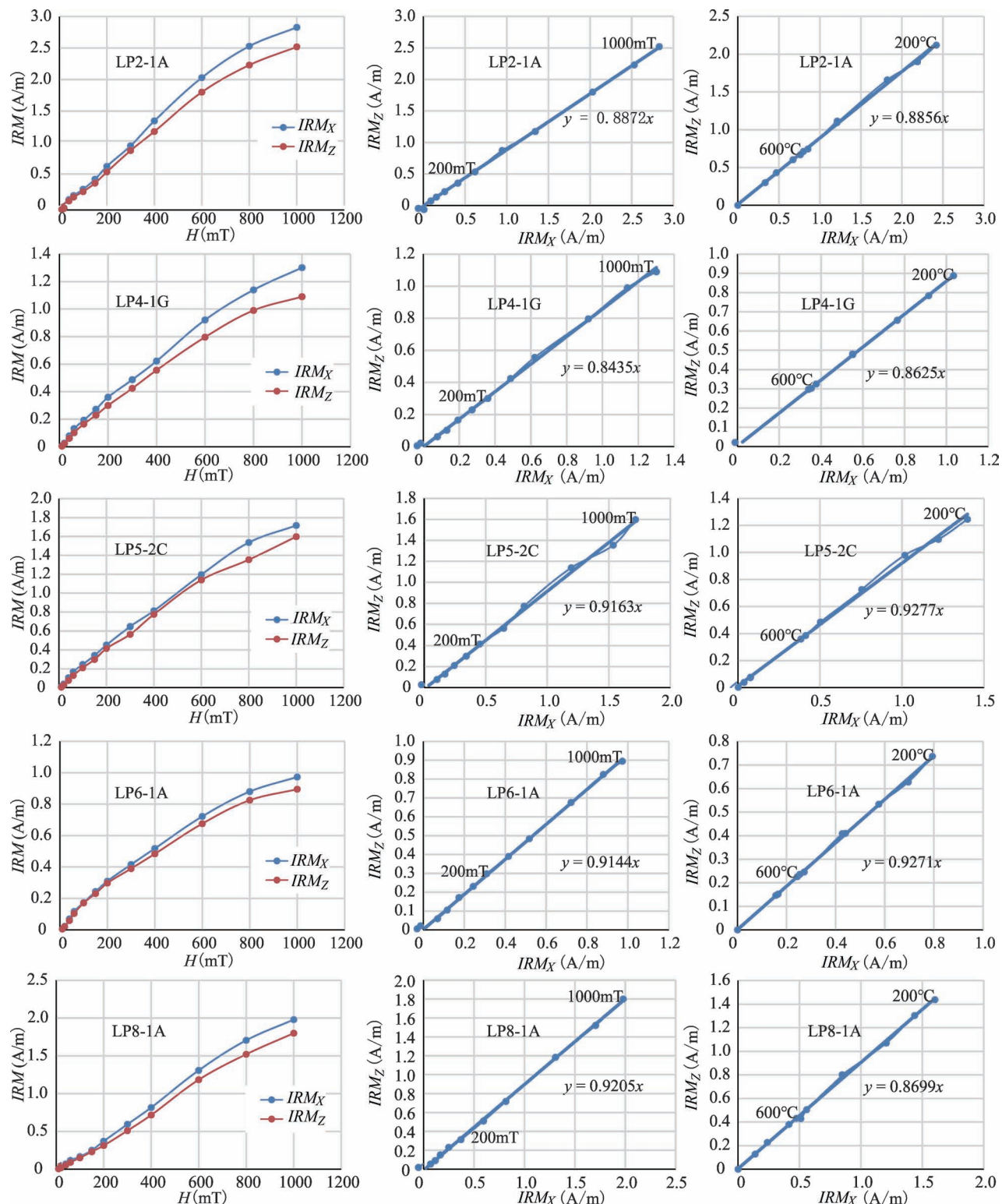


图 8 IRM_x 和 IRM_z 对比图: (a) 斜向 45° 加场过程; (b) 外加磁场强度过程 ($10 \sim 1000$ mT);
(c) 热退磁过程 ($200 \sim 690^\circ\text{C}$)

Fig. 8 Comparison diagram of IRM_x and IRM_z : (a) 45° oblique field process; (b) apply field process ($10 \sim 1000$ mT);
(c) thermal demagnetization process ($200 \sim 690^\circ\text{C}$)

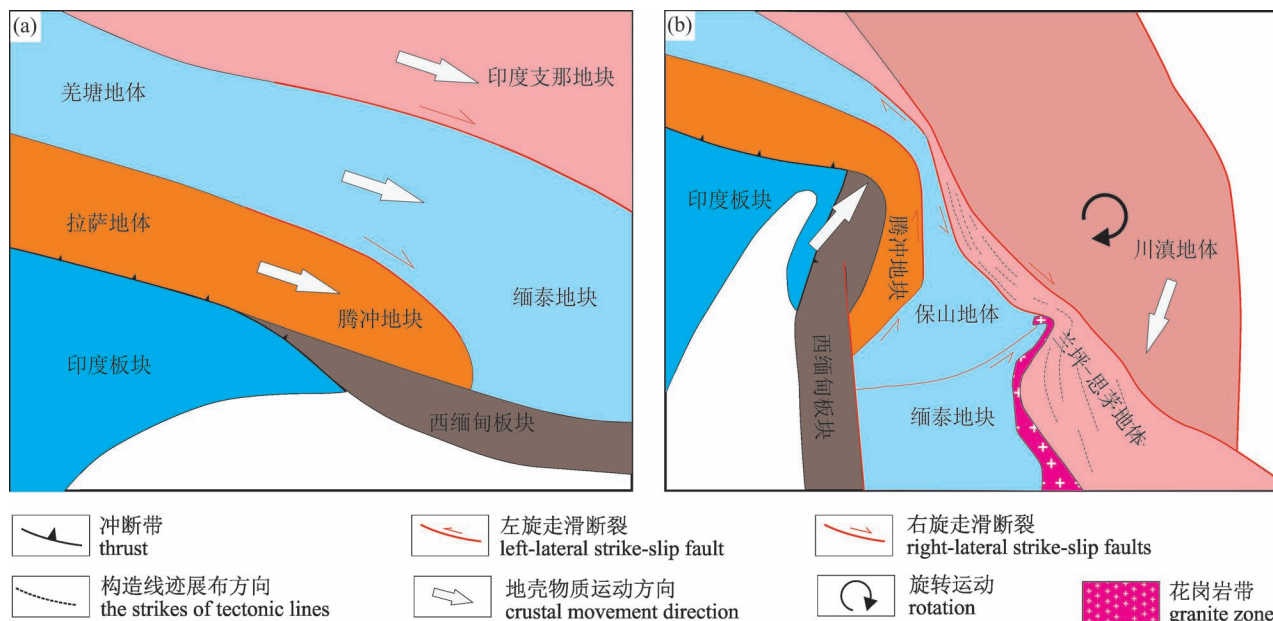


图9 兰坪—思茅地体差异性旋转变形的构造模型: (a) 受印亚碰撞影响, 在渐新世早期至早中新世, 青藏高原东南缘地壳物质开始发生侧向挤出运动; (b) 自中中新世以来, 由于东喜马拉雅构造节的楔入, 川滇地体的南向挤压及临沧—勐连花岗岩带的阻挡作用, 兰坪—思茅地体在整体侧向旋转挤出的基础上, 内部发生与地壳构造变形相关的差异性旋转变形

Fig. 9 Tectonic model of differential rotational deformation of Lanping Simao terrane: (a) The crustal materials of the southeastern edge of Xizang (Tibetan) began to southeastward extrusion movement during the early Oligocene to early Miocene; (b) Since the middle Miocene, the internal of Lanping—Simao terrane experienced different rotation movement related to the regional crustal deformation on the basis of the integrated lateral rotational extrusion, due to the wedging of Eastern Himalaya Syntaxis, the southward compression of the Chuandian terrane and the obstruction of the Lincang granite belt

转基础上进一步叠加了局部的地壳顺时针旋转变形。而地体中部地区由于受川滇地体的南向挤压, 以及临沧花岗岩带的阻挡作用, 而发生了局部的地壳构造变形, 从而导致这一区域叠加了复杂的差异性旋转变形(图9a,b)。至于兰坪—思茅地体与其西南侧保山地体和腾冲地体之间存在的新生代差异性纬向运移的原因, 还需要在保山地体和腾冲地体内进行更为深入和精细的古地磁学研究。

5 结论

(1) 兰坪—思茅地体北部兰坪盆地始新世红层中获得的原生特征剩磁结果为 $D_s = 264.5^\circ$, $I_s = -39.4^\circ$, $k = 21.4$, $\alpha_{95} = 9.6^\circ$, 表明自晚始新世以来, 兰坪—思茅地体北部相对于东亚古地磁参考极发生了 $80.3^\circ \pm 8.9^\circ$ 的顺时针旋运动。与保山地体和腾冲地体晚渐新世—早中新世以来发生的顺时针旋转量保持一致。磁倾角偏低的数据仍显示, 兰坪盆地相对于东亚稳定地区经历了 $5.8^\circ \pm 7.2^\circ$ (638 ± 792 km) 的不显著南向运移, 这表明兰坪—思茅地

体北部和中部自晚始新世以来的确存在差异性的纬向运动。

(2) 兰坪—思茅地体北部所受应力随着东喜马拉雅构造节的北北东向推进, 逐渐由北东向转变为北东东向, 这一应力场变化致使北部地区上地壳持续发生北东—南西向的缩短和北西—南东向的韧性伸展, 从而导致该地区南向位移量小于中南部。这种地壳运动趋势表明, 上地壳沿大型走滑断裂带发生的东南向挤出逃逸运动和下地壳通道流所导致的上地壳韧性变形作用在兰坪—思茅地体东南向逃逸过程中共存。但是, 兰坪—思茅地体北部较大的顺时针旋转变形与印度板块东端和西缅甸地块向北楔入欧亚大陆所造成的北东—东向挤压作用相关, 而地体中部复杂的差异性旋转变形与川滇地体的南向挤压和临沧花岗岩带的阻挡作用所导致的局部地壳构造变形相关。

致谢:自然资源部古地磁与古构造重建重点实验室及其他成员在样品测试和分析中给予了指导和帮助,在此表示诚挚的谢意。

参 考 文 献 / References

(The literature whose publishing year followed by a “&” is in Chinese with English abstract; The literature whose publishing year followed by a “#” is in Chinese without English abstract)

- 安纯志, 杨振宇, 全亚博, 李晨皓, 王恒, 高亮, 韩志锐, 徐颖超. 2017. 印支地块思茅地区始新统磁倾角偏低现象及其构造意义. *吉林大学学报(地球科学版)*, 47(2): 511~525.
- 冯志强, 郭建秋, 阮林森, 李诗强, 玖业龙, 刘文强, 密文天. 2012. 兰坪盆地古近系宝相寺组层序地层分析. *地质找矿论丛*, 27(1): 103~108.
- 李仕虎, 黄宝春, 朱日祥. 2012. 青藏高原东南缘构造旋转的古地磁学证据. *地球物理学报*, 55(1): 76~94.
- 刘宇平, 潘桂棠, 耿全如, 郑来林, 刘朝基. 2000. 南迦巴瓦构造结的楔入及其地质效应. *沉积与特提斯地质*, 1: 52~59.
- 施小斌, 丘学林, 刘海龄, 储著银, 夏斌. 2006. 滇西临沧花岗岩基冷却的热年代学分析. *岩石学报*, 22(2): 465~479.
- 孙志明, 李兴振, 沈敢富, 杜德勋, 江新胜. 2001. 云南雪龙山韧性剪切带研究新进展. *沉积与特提斯地质*, 21(2): 48~56.
- 全亚博, 杨振宇, 王恒, 张旭东, 安纯志, 徐颖超, 赵越. 2014. 中国西南兰坪—思茅地体中部白垩纪古地磁结果及陆内变形特征. *地球物理学报*, 57(1): 179~198.
- 王二七, Burchfiel B C, 季建清. 2001. 东喜马拉雅构造节新生代地壳缩短量的估算及其地质依据. *中国科学(D辑: 地球科学)*, 31(1): 1~9.
- 徐颖超, 全亚博, 王恒, 杨振宇. 2017. 青藏高原东南缘兰坪—思茅盆地反 S 型构造属性的古地磁约束. *地质论评*, 63(3): 549~567.
- 杨振宇, Besse J, 孙知明, 赵越. 1998. 印度支那地块第三纪造滑移与青藏高原岩石圈构造演化. *地质学报*, 72(2): 112~125.
- 云南省地质矿产局. 1990. 云南省区域地质志. 北京: 地质出版社: 1~728.
- 张海峰, 全亚博, 王恒, 杨振宇. 2012. 印支地体兰坪—思茅地区早白垩世古地磁结果及其构造意义. *地质学报*, 86(6): 923~939.
- 张进江, 钟大赉, 季建清, 丁林, 桑海清. 2001. 东喜马拉雅构造节大陆碰撞以来构造年代学框架及其与哀牢山—红河构造带的对比. *矿物岩石地球化学通报*, 20(4): 243~244.
- 张岳桥, 董树文, 侯春堂, 石菊松, 吴中海, 李海龙, 孙萍, 刘刚, 李建. 2013. 四川芦山 2013 年 Ms7.0 地震发震构造初步研究. *地质学报*, 87(6): 747~758.
- 张岳桥, 杨农, 施炜, 董树文. 2008. 青藏高原东缘新构造及其对汶川地震的控制作用. *地质学报*, 82(12): 1668~1678.
- 朱志军, 姜勇彪, 郭福生, 侯增谦, 杨天南, 薛传东. 2011. 兰坪盆地古近纪沉积相类型及沉积环境演化. *岩石矿物学杂志*, 30(3): 409~418.
- Akciz S, Burchfiel B C, Crowley J L, Yin Jiyun, Chen Liangzhong. 2008. Geometry, kinematics, and regional significance of the Chong Shan shear zone, Eastern Himalayan Syntaxis, Yunnan, China. *Geosphere*, 4(1): 292~314.
- An Chunzhi, Yang Zhenyu, Tong Yabo, Li Chenhao, Wang Heng, Gao Liang, Han Zhirui, Xu Yingchao. 2017&. Eocene paleomagnetic inclination shallowing in simao area of the indochina block and its tectonic implication. *Journal of Jilin University (Earth Science Edition)*, 47(2): 511~525.
- Beck R A, Durbank D W, Sercombe W J, Riley G W, Barndt J K, Jurgen H, Metje J, Cheema A, Shafique N A, Lawrence R D, Khan M A. 1995. Stratigraphic evidence for an early collision between northwest India and Asia. *Nature*, 373: 55~58.
- Burg J P, Nievergelt P, Oberli F, Seward D, Meier M. 1998. The namche barwa syntaxis: evidence for exhumation related to compressional crustal folding. *Journal of Asian Earth Sciences*, 16: 239~252.
- Butler R F. 1998. Paleomagnetism: Magnetic domains to geologic Terranes (electronic ed). Tucson A Z, Department of Geosciences, 238.
- Cao Yong, Sun Zhiming, Li Haibing, Pei Junling, Jiang Wan, Xu Wei, Zhao Laishi, Wang Leizhen, Li Chenglong, Ye Xiaozhou, Zhang Lei. 2017. New Late Cretaceous paleomagnetic data from volcanic rocks and red beds from the Lhasa terraneand itsimplications forthe paleolatitude ofthe southern marginof Asia prior tothe collision with India. *Gondwana Research*, 41: 337~351.
- Chen Haihong, Dobson J, Heller F, Jie Hao. 1995. Paleomagnetic evidence for clockwise rotation of the Simao region since the Cretaceous: a consequence of India—Asia collision. *Earth and Planetary Science Letters*, 134(1~2): 203~217.
- Chung Sunlin, Lee Tungyi, Lo Chinghua, Wang Peiling, Chen Chin Yu, Yem Nguyentrong, Hoa Nguyentrong, Wu Genyao. 1997. Intraplate extension prior to continental extrusion along the Ailao Shan Red River shear zone. *Geology*, 25(4): 311~314.
- Clark M, Royden L. 2000. Topographic ooze: building the eastern margin of Tibet by lower crustal flow. *Geology*, 28(8): 703~706.
- Cogné J P, Besse J, Chen Yan, Hankard F. 2013. A new Late Cretaceous to Present APWP for Asia and its implications for paleomagnetic shallow inclinations in Central Asia and Cenozoic Eurasian plate deformation. *Geophysical Journal International*, 192(3): 1000~1024.
- Copley A, Avouac J P, Royer J Y. 2010. India—Asia collision and the Cenozoic slowdown of the Indian plate: implications for the forces driving plate motions. *Journal of Geophysical Research*, 115: B03410.
- Dewey J F, Shackleton R M, Chang Chengfa, Sun Yiyin. 1988. The tectonic evolution of the Tibetan Plateau. *Philosophical Transactions of The Royal Society B Biological Sciences*, 327(1594): 379~413.
- Dupont-Nivet G, Lippert P C, van Hinsbergen D J J, Meijers M J M, Kapp P. 2010. Palaeolatitude and age of the Indo—Asia collision: palaeomagnetic constraints. *Geophysical Journal International*, 182: 1189~1198.
- Feng Zhiqiang, Gou Jianqiu, Ruan Linsen, Li Shiqiang, Mou Yelong, Liu Wenqiang, Mi Wentian. 2012&. Sequence stratigraphy analysis of paleogene baoxiangsi formation in lanping basin. *Contributions to Geology and Mineral Resources Research*, 27(1): 103~108.
- Fisher R A. 1953. Dispersion on a sphere. *Proceedings of the Royal Society A: Mathematical, Physical and Engineering Sciences*, 217(1130): 295~305.
- Funahara S, Nishiwaki N, Miki M, Murata F, Otofuji Y, Wang Yizhao. 1992. Paleomagnetic study of Cretaceous rocks from the Yangtze block, central Yunnan, China: implications for the India—Asia collision. *Earth and Planetary Science Letters*, 113(1~2): 77~91.
- Funahara S, Nishiwaki N, Murata F, Otofuji Y, Wang Yizhao. 1993. Clockwise rotation of the Red River fault inferred from paleomagnetic study of Cretaceous rocks in the Shan—Thai—Malay Block of western Yunnan, China. *Earth and Planetary Science Letters*, 117: 29~42.

- Gao Liang, Yang Zhenyu, Tong Yabo, Wang Heng, An Chunzhi. 2015. New paleomagnetic studies of Cretaceous and Miocene rocks from Jinggu, western Yunnan, China: Evidence for internal deformation of the Lanping—Simao Terrane. *Journal of Geodynamics*, 89: 39~59.
- Gilley L D, Harrison T M, Leloup P H, Ryerson F J, Lovera O M, Wang Jianghai. 2003. Direct dating of left-lateral deformation along the Red River shear zone, China and Vietnam. *Journal of Geophysical Research*, 108 (B2): 2127.
- Halls H C. 1976. A least-squares method to find a remanence direction from converging remagnetization circles. *Geophysical Journal of the Royal Astronomical*, 45: 297~304.
- Halls H C. 1978. The use of converging remagnetization circles in palaeomagnetism. *Physics of the Earth and Planetary Interiors*, 16: 1~11.
- Harrison T M, Copeland P, Kidd W S F, Yin An. 1992. Rising Tibet. *Science*, 255: 1663~1670.
- Hirt A M, Lowrie W. 1988. Paleomagnetism of the Umbrian—Marches orogenic belt. *Tectonophysics*, 146(1~4): 91~103.
- Hodych J P, Buchan K L. 1994. Early Silurian palaeolatitude of the Springdale Group redbeds of central Newfoundland: a palaeomagnetic determination with a remanence anisotropy test for inclination error. *Geophysical Journal International*, 117(3): 640~652.
- Huang Baochun, Piper J D A, Wang Yongcheng, He Huaiyu, Zhu Rixiang. 2005. Paleomagnetic and geochronological constraints on the postcollisional northward convergence of the southwest Tian Shan, NW China. *Tectonophysics*, 409(1~4): 107~124.
- Huang Kainian, Opdyke N D. 1993. Paleomagnetic results from Cretaceous and Jurassic rocks of South and Southwest Yunnan: evidence for large clockwise rotations in the Indochina and Shan—Thai—Malay Terranes. *Earth and Planetary Science Letters*, 117(3~4): 507~524.
- King R F. 1955. The remanent magnetism of artificially deposited sediments. *Geophysical Journal International*, 7: 115~134.
- Kirschvink J L. 1980. The least-squares line and plane and the analysis of paleomagnetic date. *Geophysical Journal International*, 62(3): 699~718.
- Klootwijk C T, Conaghan P J, Powell C M. 1985. The Himalayan Arc: large-scale Continental subduction, oroclinal bending and back-arc spreading. *Earth and Planetary Science Letters*, 75(2): 167~183.
- Kodama K P. 2012. Paleomagnetism of Sedimentary Rocks: Process and Interpretation. Oxford: John Wiley and Sons, Ltd; 1~253.
- Kondo K, Mu Chuanlong, Yamamoto T, Zaman H, Miura D, Yokoyama M, Ahn H S, Otofuji Y. 2012. Oroclinal origin of the Simao Arc in the Shan—Thai Block inferred from the Cretaceous palaeomagnetic data. *Geophysical Journal International*, 190(1): 201~216.
- Kornfeld D, Eckert S, Appel E, Ratschbacher L, Pfänder A, Liu Deliang, Ding Lin. 2014b. Clockwise rotation of the Baoshan block due to southeastward tectonic escape of Tibetan crust since the Oligocene. *Geophysical Journal International*, 197(1): 149~163.
- Kornfeld D, Eckert S, Appel E, Ratschbacher L, Sonntag B L, Pfänder J A, Ding Lin, Liu Deliang. 2014a. Cenozoic clockwise rotation of the Tengchong block, southeastern Tibetan Plateau: A paleomagnetic and geochronologic study. *Tectonophysics*, 628: 105~122.
- Kruiver P P, Dekkers M J, Heslop D. 2001. Quantification of magnetic coercivity components by the analysis of acquisition curves of isothermal remanent magnetisation. *Earth and Planetary Science Letters*, 189(3~4): 269~276.
- Lee T Y, Lawver L A. 1995. Cenozoic plate reconstruction of Southeast Asia. *Tectonophysics*, 251(1~4): 85~138.
- Leloup P H, Amaud N, Lacassin R, Kienast J R, Harrison T M, Phan Trong T T, Replumaz A, Tappognier P. 2001. New constraints on the structure, thermochronology, and timing of the Ailao Shan—Red River shear zone, SE Asia. *Journal of Geophysical Research*, 106(B4): 6683~6732.
- Leloup P H, Lacassin R, Tappognier P, Zhong Dalai, Lui Xiaohan, Zhang Liangshang, Ji Shaocheng. 1995. The Ailao Shan—Red River shear zone (Yunnan, China), Tertiary transform boundary of Indochina. *Tectonophysics*, 251(1): 3~84.
- Li Shihu, Advokaat E L, van Hinsbergen D J J, Koymans M, Deng Chenglong, Zhu Rixiang. 2017. Paleomagnetic constraints on the Mesozoic—Cenozoic paleolatitudinal and rotational history of Indiana and South China: review and updated kinematic reconstruction. *Earth-Science Reviews*, 171: 58~77.
- Li Shihu, Deng Chenglong, Dong Wei, Sun Lu, Liu Suzhen, Qin Huafeng, Yin Jijun, Ji Xueping, Zhu Rixiang. 2015. Magnetostriatigraphy of the Xiaolongtan Formation bearing *Lufengpithecus keiyuanensis* in Yunnan, southwestern China: constraint on the initiation time of the southern segment of the Xianshuihe—Xiaojiang fault. *Tectonophysics*, 655: 213~226.
- Li Shihu, Huang Baochun, Zhu Rixiang. 2012&. Paleomagnetic constraints on the tectonic rotation of the southeastern margin of the Tibetan Plateau. *Chinese Journal of Geophysics*, 55(1): 76~94.
- Li Zhenyu, Ding Lin, Song Peiping, Fu Jiajun, Yue Yahui. 2015. Paleomagnetic constraints on the paleolatitude of the Lhasa Terrane during the Early Cretaceous: implications for the onset of India—Asia collision and latitudinal shortening estimates across Tibet and stable Asia. *Gondwana Research*, 41: 352~372.
- Licht A, Dupont-Nivet G, Win Z, Swe H H, Kaythi M, Roperch P, Ugrai T, Littell V, Park D, Westerweel J, Jones D, Poblete F, Aung D W, Huang Huasheng, Hoorn C, Sein K. 2018. Paleogene evolution of the Burmese forearc basin and implications for the history of India—Asia convergence. *Geological Society of America Bulletin*, 131: 730~748.
- Liebke U, Appel E, Ding Lin, Neumann U, Antolin B, Xu Qiang. 2010. Position of the Lhasa terrane prior to India—Asia collision derived from paleomagnetic inclinations of 53 Ma old dykes of the Linzhou Basin: constraints on the age of collision and post-collisional shortening within the Tibetan Plateau. *Geophysical Journal International*, 182(3): 1199~1215.
- Liu Yuping, Pan Guitang, Geng Quanru, Zheng Lailin, Liu Chaoji. 2000&. The wedging of the Namjagbarwa syntaxis in southeastern Xizang and its geological effects. *Sedimentary Geology and Tethyan Geology*, 1: 52~59.
- Lowrie W. 1990. Identification of ferromagnetic minerals in a rock coercivity and unblocking temperature properties. *Geophysical Journal International*, 17(2): 159~162.
- Ma Yiming, Yang Tianshui, Yang Zhenyu, Zhang Shihong, Wu Huachun, Li Haiyan, Li Huikun, Chen Weiwei, Zhang Junhong, Ding Jikai. 2014. Paleomagnetism and U-Pb zircon geochronology of Lower Cretaceous lava flows from the western Lhasa terrane: new constraints on the India—Asia collision process and intracontinental deformation within Asia. *Journal of Geophysical Research: Solid Earth*, 119(10): 7404~7424.

- Maurin T, Rangin C. 2009. Structure and kinematics of the Indo—Burmese wedge: Recent and fast growth of the outer wedge. *Tectonics*, 28: TC20010.
- McFadden P L. 1990. A new fold test for paleomagnetic studies. *Geophysical Journal International*, 103(1): 163~169.
- Molnar P, Dayem K E. 2010. Major intracontinental strike-slip faults and contrasts in lithospheric strength. *Geosphere*, 6 (4): 444 ~ 467.
- Molnar P, Stock J M. 2009. Slowing of India's convergence with Eurasia since 20 Ma and its implications for Tibetan mantle dynamics. *Tectonics*, 28(3): TC3001.
- Molnar P, Tapponnier P. 1975. Cenozoic tectonics of Asia: effects of a continental collision. *Science*, 189: 419~426.
- Morley C K, Arboit F. 2019. Dating the onset of motion on the Sagaing fault: Evidence from detrital zircon and titanite U-Pb geochronology from the North Minwun Basin, Myanmar. *Geology*, 47: 1~5.
- Najman Y, Appel E, Boudagher-Fadel M, Brown P, Carter A, Garzanti E, Godin L, Han J, Liebke U, Oliver G, Parrish R, Vezzoli G. 2010. Timing of India—Asia collision: geological, biostratigraphic, and paleomagnetic constraints. *Journal of Geophysical Research: Solid Earth*, 115 (B12).
- Otofuji Y, Tung V D, Fujihara M, Tanaka M, Yokoyama M, Kitada K, Zaman H. 2012. Tectonic deformation of the southeastern tip of the Indochina Peninsula during its southward displacement in the Cenozoic time. *Gondwana Research*, 22(2): 615~627.
- Özdemir Ö, Dunlop D J. 1993. Chemical remanent magnetization during γfeoo phase transformations. *Journal of Geophysical Research: Solid Earth*, 98(B3): 4191~4198.
- Peltzer G, Tapponnier P. 1988. Formation and evolution of strike-slip faults, rifts, and basins during the India—Asia collision: an experimental approach. *Journal of Geophysical Research*, 93 (B12): 15085~15117.
- Replumaz A, Tapponnier P. 2003. Reconstruction of the deformed collision zone between India and Asia by backward motion of lithospheric blocks. *Journal of Geophysical Research*, 108 (B6): 2285. <http://dx.doi.org/10.1029/2001JB000661>.
- Roger F, Calassou S, Lancelot J, Malavieille J, Mattauer M, Xu Zhiqin, Hao Ziwen, Hou Liwei. 1995. Miocene emplacement and deformation of the Konga-Shan granite (Xianshui-He fault zone, West Sichuan, China)—geodynamic implications. *Earth and Planetary Science Letters*, 130(1~4): 201~216.
- Royden L H, Burchfiel B C, Vander Hilst R D. 2008. The geological evolution of the Tibetan Plateau. *Science*, 321 (5892): 1054 ~ 1058.
- Sato K, Liu Yanyu, Wang Yongbiao, Yokoyama M, Yoshioka S, Yang Zhenyu, Otofuji Y. 2007. Paleomagnetic study of Cretaceous rocks from Pu'er, western Yunnan, China: evidence of internal deformation of the Indochina block. *Earth and Planetary Science Letters*, 258(1): 1~15.
- Sato K, Liu Yanyu, Zhu Zhicheng, Yang Zhenyu, Otofuji Y. 1999. Paleomagnetic study of Middle Cretaceous rocks from Yunlong, Western Yunnan, China: evidence of southward displacement of Indochina. *Earth and Planetary Science Letters*, 165(1): 1~15.
- Sato K, Liu Yanyu, Zhu Zhicheng, Yang Zhenyu, Otofuji Y. 2001. Tertiary paleomagnetic data from northwestern Yunnan, China: further evidence for large clockwise rotation of the Indochina block and its tectonic implications. *Earth and Planetary Science Letters*, 185(1): 185~198.
- Schwartz S Y, Voo R V D. 1983. Paleomagnetic evaluation of the orocline hypothesis in the central and southern Appalachians. *Geophysical Research Letters*, 10(7): 505~508.
- Schwartz S Y, Voo R V D. 1984. Paleomagnetic study of thrust sheet rotation during foreland impingement in the Wyoming—Idaho overthrust belt. *Journal of Geophysical Research: Solid Earth*, 89 (B12): 10077~10086.
- Searle M. 2006. Role of the Red River shear zone, Yunnan and Vietnam, in the continental extrusion of SE Asia. *Journal of the Geological Society*, 163: 1025~1036.
- Shen Zhenkang, Lu Jiangning, Wang Min, Burgmann R. 2005. Contemporary crustal deformation around the southeast borderland of the Tibetan Plateau. *Journal of Geophysical Research*, 110: B11409.
- Shi Xiaobin, Qiu Xuelin, Liu Hailing, Chu Zhuyin, Xia Bin. 2006&. Thermochronological analyses on the cooling history of the Lincang Granitoid Batholith, Western Yunnan. *Acta Petrologica Sinica*, 22 (2): 465~479.
- Sun Zhiming, Li Xingzhen, Shen Ganfu, Du Dexun, Jiang XinSheng. 2001&. Advances in the research on the Xuelongshan ductile shear zone in Yunnan. *Sedimentary Geology and Tethyan Geology*, 21 (2): 48~56.
- Tan Xiaodong, Kodama K P, Chen Hanlin, Fang Dajun, Sun Dongjiang, Li Yongan. 2003. Paleomagnetism and magnetic anisotropy of Cretaceous red beds from the Tarim basin, northwest China; evidence for a rock magnetic cause of anomalously shallow paleomagnetic inclinations from central Asia. *Journal of Geophysical Research*, 108 (B2). <http://dx.doi.org/10.1029/2001jb001608>.
- Tan Xiaodong, Kodama K P, Fand Dajun. 1996. A preliminary study of the effect of compaction on the redeposited haematite-bearing sediments disaggregated from Eocene red beds from the Tarim basin, northwest China. *Eos, Transactions of the American Geophysical Union*, 77(46) (Fall Meet. Suppl, F155).
- Tanaka K, Mu Chuanlong, Sato K, Takemoto K, Miura D, Liu Yuyan, Zaman H, Yang Zhenyu, Yokoyama M, Iwamoto H, Uno K, Otofuji Y. 2008. Tectonic deformation around the eastern Himalayan syntaxis: constraints from the Cretaceous palaeomagnetic data of the Shan—Thai Block. *Geophysical Journal of the Royal Astronomical Society*, 175(2): 713~728.
- Tapponnier P, Peltzer G, Armijo R. 1986. On the mechanics of the collision between India and Asia. *Geological Society, London, Special Publications*, 19(1): 113~157.
- Tapponnier P, Peltzer G, Le Dain A Y, Armijo R, Cobbold P. 1982. Propagating extrusion tectonics in Asia: new insights from simple experiments with plasticine. *Geology*, 10(12): 611~616.
- Tapponnier P, Xu Zhiqin, Roger F, Mayer B, Arnaud N, Wittlinger G, Yang Jingsui. 2001. Oblique stepwise rise and growths of the Tibet Plateau. *Science*, 294(5547): 1671~1677.
- Tauxe L, Kent D V. 2004. A simplified statistical model for the geomagnetic field and the detection of shallow bias in paleomagnetic inclinations: was the ancient magnetic field dipolar? *American Geophysical Union*, 154: 101~115.
- Tauxe L. 2005. Inclination flattening and the geocentric axial dipole hypothesis. *Earth and Planetary Science Letters*, 233(3~4): 247~261.
- Thébault E, Finlay C, Beggan C, Alken P, Aubert J, Barrois O, Bertrand F, Bondar T, Boness A, Brocco L, Daix Canet E, Chambodut A, Chulliat A, Coiffson P, Civet F, Du A, Fournier A,

- Fratter I, Gillet N, Zvereva T. 2015. International Geomagnetic Reference Field: the 12th generation. *Earth, Planets, and Space*, 67: 79. <https://doi.org/10.1186/s40623-015-0228-9>.
- Tong Yabo, Yang Zhenyu, Jing Xianqing, Zhao Yue, Li Chenhao, Huang Dianjun, Zhang Xudong. 2016. New insights into the Cenozoic lateral extrusion of crustal blocks on the southeastern edge of Tibetan Plateau: Evidence from paleomagnetic results from Paleogene sedimentary strata of the Baoshan Terrane. *Tectonics*, 35(11): 2494~2514.
- Tong Yabo, Yang Zhenyu, Pei Junling, Wang Heng, Xu Yingchao, Pu Zongwen. 2017. Paleomagnetism of the Upper Cretaceous red-beds from the eastern edge of the Lhasa Terrane: New constraints on the onset of the India—Eurasia collision and latitudinal crustal shortening in southern Eurasia. *Gondwana Research*, 48: 86~100.
- Tong Yabo, Yang Zhenyu, Wang Heng, Gao Liang, An Chunzhi, Zhang Xudong, Xu Yingchao. 2015. The Cenozoic rotational extrusion of the Chuan Dian Fragment: New paleomagnetic results from Paleogene red-beds on the southeastern edge of the Tibetan Plateau. *Tectonophysics*, 658(2015): 46~60.
- Tong Yabo, Yang Zhenyu, Wang Heng, Zhang Xudong, An Chunzhi, Xu Yingchao, Zhao Yue. 2014&. The Cretaceous paleomagnetic results from the central part of the Simao Terrane in the southwest part of China and its tectonic implications. *Chinese Journal of Geophysics*, 57(1): 179~198.
- Tong Yabo, Yang Zhenyu, Zheng Liandi, Xu Yingchao, Wang Heng, Gao Liang, Hu Xuzhi. 2013. Internal crustal deformation in the northern part of Shan - Thai Block: new evidence from paleomagnetic results of Cretaceous and Paleogene redbeds. *Tectonophysics*, 608(2013): 1138~1158.
- Tong Yabo, Yang Zhenyu, Zheng Liandi, Yang Tianshui, Shi Linfeng, Sun Zhiming, Pei Junling. 2008. Early Paleocene Paleomagnetic results from Southern Tibet and its tectonic implication. *International Geology Review*, 50: 546~562.
- Van Hinsbergen D J J, Kapp P, Dupont-Nivet G, Lippert P C, DeCelles P G, Torsvik T H. 2011. Restoration of Cenozoic deformation in Asia and the size of Greater India. *Tectonics*, 30: TC5003. <http://dx.doi.org/10.1029/2011TC002908>.
- Van Hinsbergen D J, Lippert P C, Dupont-Nivet G, McQuarrie N, Doubrovine P V, Spakman W, Torsvik T H. 2012. Greater India Basin hypothesis and a two-stage Cenozoic collision between India and Asia. *National Academy of Sciences Proceedings*, 109: 7659~7664.
- Voo R V D, Channell J E T. 1980. Paleomagnetism in orogenic belts. *Reviews of Geophysics*, 18(2): 455~481.
- Wang E C, Burchfiel B C, Royden L H, Chen Liangzhong, Chen Jishen, Lin Wenxin, Chen Zhiliang. 1998. Late Cenozoic Xianshuihe—Xiaojiang, Red River, and Dali Fault Systems of Southwestern Sichuan and Central Yunnan, China. *Geological Society of America Special Paper*, 327: 1~108.
- Wang E C, Burchfiel B C. 2000. Late Cenozoic to Holocene deformation in southwestern Sichuan and adjacent Yunnan, China, and its role in formation of The southeastern part of the Tibetan Plateau. *Geological Society of America Bulletin*, 112(3): 413~423.
- Wang E C, Burchfiel B C, Ji Jianqing. 2001#. Estimation of Cenozoic crustal shortening in the Eastern Himalaya Syntaxis and its geological evidence. *Science in China (Series D)*, 31(1): 1~9.
- Wang Heng, Yang Zhenyu, Tong Yabo, Gao Liang, Jing Xianqing, Zhang Haifeng. 2016. Palaeomagnetic results from Palaeogene red beds of the Chuan—Dian Fragment, southeastern margin of the Tibetan Plateau: implications for the displacement on the Xianshuihe—Xiaojiang fault systems. *International Geology Review*, 58(11): 1363~1381.
- Wang Jianghai, Yin An, Harrison T M, Grove M, Zhang Yuquan, Xie Guanghong. 2001. A tectonic model for Cenozoic igneous activities in the eastern Indo—Asian collision zone. *Earth and Planetary Science Letters*, 188(1~2): 123~133.
- Wang Shifeng, Fang Xiaomin, Zheng Dewen, Wang, E. C. 2009. Initiation of slip along the Xianshuihe fault zone, eastern Tibet, constrained by K/Ar and fission-track ages. *International Geology Review*, 51(12): 1121~1131.
- Wang Yuejun, Fan Weiming, Zhang Yanhua, Peng Touping, Chen Xinyue, Xu Yigang. 2006. Kinematics and $^{40}\text{Ar}/^{39}\text{Ar}$ Archeochronology of the Gaoligong and Chongshan shear systems, western Yunnan, China: implications for early Oligocene tectonic extrusion of SE Asia. *Tectonophysics*, 418(3): 235~254.
- Watson G S, Enkin R J. 1993. The fold test in paleomagnetism as a parameter estimation problem. *Geophysical Research Letters*, 20(19): 2135~2137.
- Xu Qiang, Liu Xiaohui, Ding Lin. 2016. Miocene high-elevation landscape of the eastern Tibetan Plateau. *Geochemistry Geophysics Geosystems*, 17(10): 4254~4267.
- Xu Yingchao, Tong Yabo, Wang Heng, Yang Zhenyu. 2017&. Paleomagnetic Constraints on the Reversed S-shaped Structure Deformation of the Lanping—Simao Basin in the Southeastern Xizang (Tibet) Plateau. *Geological Review*, 63(3): 549~567.
- Yang Tianshui, Ma Yiming, Zhang Shihong, Bian Weiwei, Yang Zhenyu, Wu Huaichun, Li Haiyan, Chen Weiwei, Ding Jikai. 2015. New insights into the India—Asia collision process from Cretaceous paleomagnetic and geochronologic results in the Lhasa terrane. *Gondwana Research*, 28(2): 625~641.
- Yang Zhenyu, Besse J, Sun Zhiming, Zhao Yue. 1998&. Tertiary squeeze-out of the Indo—China block and lithospheric evolution of the Qinghai—Tibetan Plateau. *Acta Geologica Sinica*, 72(2): 112~125.
- Yang Zhenyu, Besse J. 1993. Paleomagnetic study of Permian and Mesozoic sedimentary rocks from Northern Thailand supports the extrusion model for Indochina. *Earth and Planetary Science Letters*, 117(1993): 525~552.
- Yang Zhenyu, Yin Jiyun, Sun Zhiming, Otofuji Y, Sato K. 2001. Discrepant Cretaceous paleomagnetic poles between Eastern China and Indochina: A consequence of the extrusion of Indochina. *Tectonophysics*, 334(2): 101~113.
- Yi Zhiyu, Huang Baochun, Yang Liekun, Tang Xiangde, Yan Yonggang, Qiao Qingqing, Zhao Jie, Chen Liwei. 2015. A quasi-linear structure of the southern margin of Eurasia prior to the India—Asia collision: First paleomagnetic constraints from Upper Cretaceous volcanic rocks near the western syntaxis of Tibet. *Tectonics*, 34: 1431~1451.
- Yin An, Harrison T M, Ryerson F J, Kidd W S F, Copeland P. 1994. Tertiary structural evolution of the Gangdese thrust system, southeastern Tibet. *Journal of Geophysical Research*, 99: 18175~18201.
- Yin An, Harrison T M. 2000. Geologic evolution of the Himalayan—Tibetan orogeny. *Annual Review of Earth and Planetary Science Letters*, 28: 211~280.
- Yin An. 2006. Cenozoic tectonic evolution of the Himalayan orogen as

- constrained by along-strike variation of structural geometry, exhumation history, and foreland sedimentation. *Earth-Science Reviews*, 76(1~2): 1~131.
- Zeitler P K, Meltzer A S, Koons P O, Craw D, Hallet B, Chamberlain C P, Kidd W S F, Park S K, Seeber L, Bishop M, Shroder J. 2001. Erosion, Himalayan geodynamics, and the geomorphology of metamorphism. *GSA Today*, 11: 4~8.
- Zhang Bo, Zhang Jinjiang, Zhong Dalai. 2010. Structure, kinematics and ages of transpression during strain partitioning in the Chongshan shear zone, western Yunnan, China. *Journal of Structural Geology*, 32(2010): 445~463.
- Zhang Haifeng, Tong Yabo, Wang Heng, Yang Zhenyu. 2012&. Early cretaceous paleomagnetic results of the simao area in the indochina block and its tectonic implications. *Acta Geologica Sinica*, 86(6): 923~939.
- Zhang Jinjiang, Zhong Dalai, Ji Jianqing, Ding Lin, Sang Haiqing. 2001&. The structural—chronological frame of the eastern Himalayan syntaxis since the India—Asia collision and its correlation with the Ailaoshan—Red River strucatural belt. *Bulletin of Mineralogy Petrology and Geochemistry*. 20(4): 243~244.
- Zhang Yueqiao, Dong Shuwen, Hou Chuntang, Shi jusong, Wu Zhonghai, Li Hailong, Sun Ping, Liu Gang, Li Jian. 2013&. Preliminary study on the seismotectonics of the 2013 Lushan Ms7.0 Earthquake, West Sichuan. *Acta Geologica Sinica*, 87(6): 747~758.
- Zhang Yueqiao, Yang Nong, Shi Wei, Dong Shuwen. 2008&. Neotectonics of Eastern Tibet and its control on the Wenchuan Earthquake. *Acta Geologica Sinica*, 82(12): 1668~1678.
- Zhu Zhijun, Jiang Yongbiao, Guo Fusheng, Hou Zengqian, Yang Tianman, Xue Chuandong. 2011&. Palaeogene sedimentary facies types and sedimentary environment evolution in Lanping basin. *Acta Petrologica Et Mineralogica*, 30(3): 409~418.
- Zijderveld J D A. 1967. A. C. demagnetizationof rocks: analysis of results. In: Collinson D W, Creer K M, Runcorn S K (Eds.). *Methods in Paleomagnetism*. New York: Elsevier; 254~286.

The contributing factor of differential crustal deformation of the Lanping—Simao terrane in the southeastern edge of the Xizang (Tibetan) Plateau since late Eocene

YANG Xiangdong^{1,2)}, TONG Yabo^{1,2)}, WANG Heng³⁾, PEI Junling^{1,2)}, SUN Xinxin⁴⁾, WANG Chenxu^{1,2)}, YANG Zhenyu⁴⁾

1) Institute of Geomechanics, Chinese Academy of Geological Sciences, Beijing, 100081;

2) Laboratory of Paleomagnetism and Tectonic Reconstruction, the Ministry of Land and Resources, Beijing, 100081;

3) Institute of Geology, China Earthquake Administration, Beijing, 100029;

4) College of Resources, Environment and Tourism, Capital Normal University, Beijing, 100048

Objectives: The lateral extrusion model and dynamic process of the crust in the northern part of the Indochina block are still controversial. To solve this problem, this study applied tectonic magnetism and inclination-shallowing correction on the late Eocene red beds in the Lanping basin in the southeastern Tibetan Plateau in order to discuss these key issues of continental deformation in this region.

Methods: According to the distribution of samples and the lithologic characteristics of samples, we selected three typical samples for rock magnetic experiments, and carried out stepwise thermal demagnetization experiments on the paleomagnetic specimens collected in Lanping area. Finally, we corrected the inclination by the 45° remanence anisotropy test.

Results: The directions of tilt corrected primary remanent magnetization was $D_s = 264.5^\circ, I_s = -39.4^\circ, k = 21.4, \alpha_{95} = 9.6^\circ, N = 12$ after inclination-shallowing correction. These results showed that the northern part of the Lanping—Simao terrane experienced $80.3^\circ \pm 8.9^\circ$ clockwise rotation and insignificant $5.8^\circ \pm 7.2^\circ$ (638 ± 792 km) southward displacement with reference to the paleomagnetic pole of East Asia since the late Eocene.

Conclusions: Considering other paleomagnetic results of previous studies, it was clear that there were significantly different rotational deformations between the northern and central parts of the Lanping—Simao terrane. This study discussed the dynamic process of deformation of the Lanping—Simao terrane and suggested that the $\sim 80^\circ$ clockwise rotational deformation of the northern part of the terrane is related to NE—E trending compression caused by the northward wedging of both the eastern part of the India Plate and the West Myanmar Block into Eurasia, while the complex differently rotational deformation in the middle of this terrane was related to the regional crustal deformation caused by the southward compression of the Chuandian terrane and the obstruction of the